A Review on Mechanical Behavior of Laminated Bamboo Lumber Connections

Assima Dauletbek [1], Haitao Li[1,2*], Rodolfo Lorenzo[3]

[1] College of Civil Engineering, Nanjing Forestry University, Nanjing 210037, China

[2] Joint International Research Laboratory for Bio-composite Building Materials and Structures, Nanjing Forestry University, Nanjing 210037, China

[3] University College London, London WC1E 6BT, UK.

*Corresponding author: Haitao Li, Professor, E-mail: lhaitao1982@126.com

ABSTRACT

Due to the transition of Architecture, Engineering and Construction (AEC) sector to a sustainable development, bamboo turned out to be a suitable option to conventional building materials due to its environmental friendliness and distinctive mechanical properties. Initially, it was impossible to use the original bamboo in flat applications due to its round cross-sectional shape, but engineered bamboo, in particular laminated bamboo lumber (LBL), solved this problem. Connections are one of the most important parts of building structures that are responsible for the distribution of loads and energy, ensuring the stability and safety of the structure by avoiding concentration of localized stress that can cause failures at the joints. Over the past decade, a series of experimental studies of connection performance of LBL have been conducted. In order to stimulate the use of laminated bamboo in construction industry, this article reviewed the existing published literature and described the behavior of LBL connections in terms of failure mechanisms and factors affecting the bearing capacity considering three connections categories, namely, LBL sheathing-to-framing connections, LBL dowel-type connections, and glued-in rods (GIROD) in LBL connections. According to the reviewed studies, LBL has great potential and can serve as a worthy alternative for conventional building materials. This work can provide a reference for engineering applications and future research.

KEYWORDS

Laminated bamboo lumber; connections; mechanical properties; composites

1 Introduction

Bamboo has got worldwide attention in the architecture, engineering, and construction (AEC) industry due to its sustainable characteristics [1-6]. It has a short life cycle and a high yield and can reach 30 m in height in 4 months and maximum strength in 3–8 years [7–11]. Its high carbon sequestration and low energy manufacturing help to reduce the impact on the environment compared to conventional building materials [9,12]. According to previous studies, bamboo copes well with bending and seismic loads, and its mechanical behaviour is comparable to mild steel, cast iron, aluminium alloys, and wood [9,13–20]. For instance, the tensile strength and modulus of elasticity (MOE) parallel to grain of Moso bamboo (Phyllostachys pubescens) can reach up to 309 MPa and 27.397 GPa in tension, 48–114 MPa and 3.6–11 GPa in compression, 50–132 MPa and 7.1–18.2 GPa in bending, and 15–20 MPa in shear, respectively [21–23]. It should be noted that the strength values of bamboo vary depending on the species type and moisture content [22,24–26]. Fig. 1 shows the selected mechanical properties of giant timber bamboo (Phyllostachys bambusoides) compared with conventional building materials. The data for giant timber bamboo, cast iron, aluminium alloy and structural steel are from reference [9], the data for Douglas-fir, eastern white pine, and northern red oak are from reference [27], and the data for concrete from reference [28].

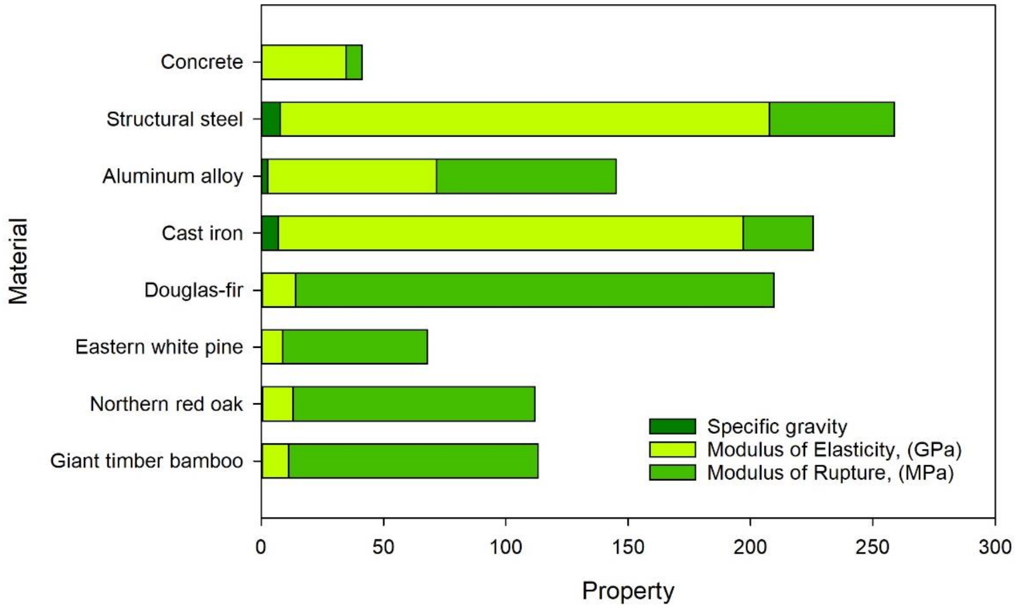

Figure 1: Selected mechanical properties of giant timber bamboo compared to conventional building materials

Due to the circular cross-section, bamboo was difficult to use in flat applications, so engineered bamboo was developed, such as laminated bamboo lumber (LBL), parallel strand bamboo (PSB), cross-laminated bamboo (CLB), glued laminated bamboo (glubam), etc. which can be utilized in various shapes and sizes, and its physical and mechanical properties are comparable to timber and glue-laminated timber products [29–36] (Fig. 2, Table 1).

(a) (b) (c)

Figure 2: Examples of engineered bamboo: (a) LBL; (b) PSB; (c) glubam.

Table 1: Selected mechanical properties of LBL material compared to similar wood and wood-based materials

Property	LBL [32, 37-41]	LVL [32, 42-44]	Glulam [43, 45, 46]	WPC [47]	Douglas Fir [42]	Teak [42, 48]
Species type	*Phyllostachys Pubescens*, *Dendrocalamus strictus*	Douglas-fir	Douglas-fir	Pine	-	-
Bending strength parallel to grain (MPa)	63.87–128.4	54.2–71.7	48.74	26.1	85	80

MOE in bending (MPa)	8320–10912	15400–19300	15370	4100	13400	9400
Tensile strength parallel to grain (MPa)	90–124	88.5	16.5–26	11.6	107.6	95–155
MOE in tension parallel to grain (MPa)	10700	13790	9400–11900	3000	11600–14800	-
Compressive strength parallel to grain (MPa)	29.55–72.60	36	24–31	28.1	49.9	41.1
MOE in compression parallel to grain (MPa)	8396–11022	-	8600	3700	-	-
Shear strength parallel to grain (MPa)	7.15–17.5	7.34	2.7–4.3	8.1	7.8	8.9

Note: LVL – laminated veneer lumber, Glulam – glued laminated timber, WPS – wood plastic composite.

As can be seen from Table 1, the strength of LBL parallel to grain was 90–124 MPa with MOE of 10700 MPa in tension, 29.55–72.60 MPa with MOE of 8396–11022 MPa in compression, 63.87– 128.4 MPa with MOE of 8320–10912 MPa in bending, and 7.15–17.5 MPa in shear [49] with the coefficient of variation (COV) within 10%. The variability in strength values of LBL can be explained by the effect of density and thickness of bamboo strips, location in culm, growth portion, type of treatment, and strips arrangements on the mechanical properties [49,50].

Over the past decade, extensive research has been done on the mechanical and physical properties of engineered bamboo. A series of studies were conducted on engineered bamboo sheathing-to-framing connections [51,52], bolted joints [53–60], roof trusses [61], and even furniture connections [62], with the results indicating that the loadcarrying capacity was comparable to timber connections. To summarize the state of the art, reviews on the existing knowledge about engineered bamboo, in particular LBL, were conducted to demonstrate its practical and potential use, as well as to increase its application in construction. Dauletbek et al. [63] reviewed the mechanical performance of structural LBL elements. Ramage et al. [64] reviewed the mechanical behaviour of bamboo scrimber and LBL and compared it to structural timber and LVL. Gatoo et al. [65] made a review of currently operating national and international timber codes and considered the possibility of developing similar comprehensive standards for LBL. Disen and Clouston [66] and Hong et al. [67] summarized the current state of the art in full culm bamboo connections.

An appropriate design of structures is a requirement of great importance, which ensures the safety of structures and the optimization of material resource consumption. According to previous studies, failure of connections is responsible for 25% of recent collapses of timber structures [68–71]. The reliability of connections is a key to stable structures, and a better understanding of the performance of the LBL connections is inevitable. This study aims to review the recent investigations on the behaviour of the LBL connections in terms of failure mechanisms and factors affecting the bearing capacity considering three connections categories, namely, LBL sheathing-to-framing connections, LBL dowel-type connections, and glued-in rods (GIROD) in LBL connections. The "Science Direct" database was used for full-text search, and 22 papers published between 2012 and 2021 were adopted for review.

2 Review on the mechanical behaviour of LBL connections

2.1 Sheathing-to-framing connections

Wooden frame buildings have always been distinguished by their high level of comfort, and resistance to extreme climatic conditions and earthquake damage. These advantages are explained by the ability of lateral systems of frame buildings to distribute energy without significant loss of lateral capacity. The lateral systems are usually wooden frames lined with wooden panels, such as oriented strand board (OSB) and plywood.

The behaviour of wood-based sheathing-to-framing connections has been thoroughly studied over the past decade. According to the studies, the material of the sheathing panel, wall aspect ratio (AR), and edge nail spacing were found to be the main influencing factors of wooden sheathing-to-framing connections' performance under lateral forces [72–79]. With the invention of LBL, recent studies have been conducted to understand the embedding strength of its connections, their mechanisms of failure, as well as factors affecting their behaviour under lateral loads. Studies were conducted both on small-size connections to understand their basic mechanical characteristics and on full-size structural shear walls and house modules to understand their potential in structural applications. Table 2 provides a summary of selected papers on small-size LBL sheathing-to-framing connections.

Table 2: Selected data on small-size LBL sheathing-to-framing connections

Nails	Size, mm	Frame	Species	Size, mm	Sheathing	Species	Density, $g.cm^{-3}$	Size, mm	Test	Edge distance, mm	Sampling number	COV, %
Self-drilling screw [80]	D 3.8, L 70	LBL	*Dendrocalamus giganteus* Munro	38×89×120	BOSB	*Dendrocalamus giganteus* Munro	0.73	12×50×300	Monotonic, cyclic	50	6 monotonic, 4 cyclic	10.54–33.09
Wire nail [80]	D 3, 3.4; L 70, 80	LBL	*Dendrocalamus giganteus* Munro	38×89×120	BOSB	*Dendrocalamus giganteus* Munro, poplar, larch	0.73, 0.63	12×50×300	Monotonic, cyclic	10, 25, 50	6 monotonic, 4 cyclic	5.54–33.76
Wire nail [81]	D 3.2; L 75	LBL	*Phylostachis pubescens* Moso	38×142.5×2464	OSB	Douglas Fir	-	11.9×50×50	Monotonic	19	11 for each geometry	32–35
Staple nail [82]	D 1.98; L 51	Wood lumber	SPF	38×89	Plybamboo	*Guadua angustifolia* Kunth	0.847	-	Monotonic, cyclic	60, 50	10 monotonic, 1 cyclic	9.97–40.94
Wire nail [82]	D 2.10; L 51	Wood lumber	SPF	38×89	Plybamboo	*Guadua angustifolia* Kunth	0.847	-	Monotonic, cyclic	60, 50	10 monotonic, 1 cyclic	8.05–30.91
Wire nail [83]	D 3.8, 4.19; L 76.2, 88.9	LBL	*Guadua angustifolia* Kunth	40×90×150	3-plybamboo	*Guadua angustifolia* Kunth	-	16×200×400	Monotonic, cyclic	19	5 monotonic tests, 10 cyclic	9.6–48.0

Notes: BOSB – bamboo-oriented strand board, OSB – oriented strand board, SPF – spruce-pine-fir lumber; L – length, D – diameter

Sun et al. [80] investigated the behaviour of bamboo-oriented strand board (BOSB) and LBL connection with different nail types and compared it to conventional OSB-LBL and plywood-LBL connections. The monotonic tests were conducted according to the ASTM D1761 [84] and 6 replicates were tested, while cyclic tests were conducted based on ISO 16670 and 4 replicates were tested [85]. According to the results, the BOSB-LBL connection showed the following failure modes: brittle failure for hex head self-tapping screw; nail yielding followed by withdrawal and partial nail head pulling trough framing member for wire nails. It was obvious, that the nail type affected the failure pattern of the BOSB-LBL connection. The specimens with an edge distance of 10 mm failed in sheathing edge-tear, while 25 and 50 mm specimens were characterized by nail withdrawal and partial nail head pulling through the framing member. Considering the effect of nails type, and edge distances, the hex-head self-tapping screw had lower deforming ability but stronger lateral resistance and stiffness than that of wire nails, and an increase in edge distances appeared to enhance the strength and ultimate displacement of specimens. However, this conclusion needs further investigation, because the size and number of the specimens were small which led to high COV values constituting 15–30%. The authors mentioned, that the tests were conducted to obtain preliminary parameters of the bamboo-based sheathing-to-framing connection. Therefore, it is necessary to conduct more tests on at least 10 replications for each variable to obtain statistically significant results. Considering the sheathing type, the BOSB-LBL connections failed by nail withdrawal and nail head pulling through BOSB, while OSB/plywood-LBL connections – by nail head pulling through the framing member and nail bending [80,82]. The authors concluded that the behaviour of the BOSBLBL connections had better lateral load-carrying capacity and energy dissipation compared to those of wood-based connections [81].

Based on test methods used for wood products, Echeverry and Correal [83] evaluated the monotonic and cyclic performance of a nailed lateral system consisting of LBL framing members and sheathing panels made of Laminated Guadua Mats (LGM) both parallel and perpendicular to the fibre direction [86] (Fig. 3).

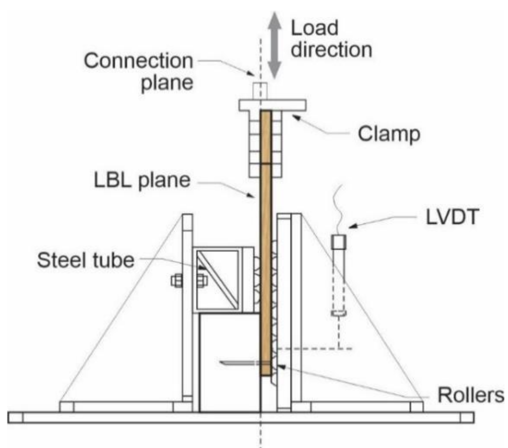

Figure 3: Test setup for LGM sheathing-to-framing connection (reproduced from [86])

The study adopted 5 monotonic tests and 10 cyclic tests for each combination of sheathing orientation and nail size to obtain preliminary but adequate results to access the variability of the experimental outcomes. According to the test results, in both monotonic and cyclic tests, the most frequent failure mode was the nail yielding in bending despite the nail size and the orientation of the sheathing panel, except for specimens with 16D nails and perpendicularly oriented panels, which failed due to partial pulling out of the nail head through the panels. In contrast to the previous study with BOSB-LBL connection, no failures due to nail withdrawal from the framing member or fatigue occurred. The authors concluded, that the orientation of panels didn’t affect the cyclic behaviour of the connection, and maximum load and displacement significantly increased with an increase in nail size. The authors found, that general cyclic behaviour and the capacity of wood-framed connections made of wood framing members (Pinus radiata D. Don) and plywood sheathing with an equivalent thickness was similar to LGM connections, showing the same failure mode as nail yielding in bending, regardless of the panel orientation or nail size. Wood connections appeared to be more ductile since the monotonic load–displacement values were 20–35% higher than those of LGM connections. The lower stiffness of LGM connections can be explained by the nonuniform density of the material caused by voids and imperfections of the split Guadua mats. Therefore, the optimization of manufacturing LGM panels should ensure the improvement of its connection capacity. In addition, further research should be done to investigate the behaviour of propersize LGM shear walls following the recommendation of international standards.

Sinha and Miyamoto [81] compared plate (PG) and edge (EG) geometries of LBL-OSB connections loaded perpendicular and parallel to LBL (Fig. 4).

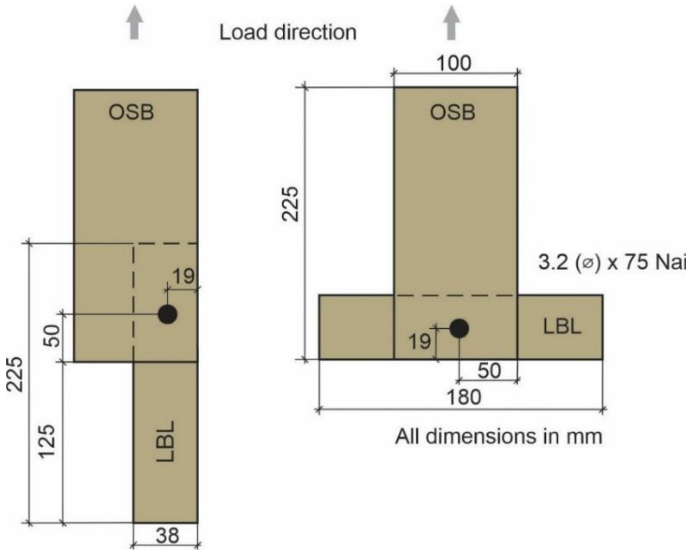

(a) (b)

Figure 4: Schematic of connection geometries: (a) edge connection; (b) plate connection [81]

A total of 22 connections were tested, 11 for each geometry. According to the results, no statistically significant differences were observed in the strength of both geometries. The authors used National Design Specification (NDS) Yield Model [87] for the design of nailed connections and concluded that it could reasonably predict capacity and yielding mode for EG if the dowel-bearing capacity of the material was known. However, the model overestimated the values for PG. In addition, the observed COV for EG and PG connections were 35% and 32%, respectively, and the number of samples tested in this study statistically confirmed the obtained results only at an 80% confidence level. Therefore, further investigation is necessary for the estimation of PG and LBL-OSB connections of different sizes.

The behaviour of bamboo-based sheathing-to-framing connections has also been studied in view of the structural applications, where members have been used in real dimensions. Table 3 provides the details from selected studies on sheathing-to-framing connections with structural dimensions. The material of sheathing panels was represented by Glued Laminated Guadua (GLG) connected to framing members made of wood or LBL

Table 3: Selected data on bamboo-based sheathing-to-framing connections with structural dimensions

Nails	D, mm	Length, mm	Frame	Species	Size, mm	Sheathing	Size, mm	AR	Loading	Edge distance, mm	Sampling number
Wire nail [88]	3.05	63.5	Wood, solid	Chilean Radiata pine	41×90	GLG	9×1200×2400	1:1, 2:1	Monotonic, cyclic	152	24

Wire nail [89]	3.05	63.5	Wood, solid	Chilean Radiata pine	41×90	GLG	9×1200×2400	1:1, 2:1	Monotonic, cyclic	51, 76, 152	3
Bolts [90]	9.5	-	GLG, box section	*Guadua angustifolia* Kunth	100×100	GLG	15×200×1300	-	Lateral	-	3
Bolts [90]	9.5	-	GLG, box section, K-bracing	*Guadua angustifolia* Kunth	100×100	No panels	-	-	Lateral	-	3

Correal and Varela [89] examined and compared 3 building modules as one-story module, a two-story module, and a two-story module with a wall finish, the shear walls of which were made of GLG, OSB, and plywood. Under the shake table test, the modules exhibited light damage on the wall and the wooden frame structure without finishing, and significant cracking appeared on the corners of the windows and at the joints between the structural and non-structural walls of the exterior and interior finishing (Fig. 5).

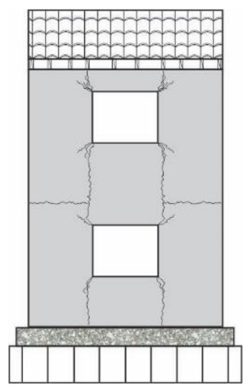

Figure 5: Cracking pattern in exterior stucco after the tests [89]

Varela et al. [88] compared the cyclic performance of shear walls made of LBL, OSB, and Plywood with different edge nail spacing of 50 mm, 76 mm, and 152 mm and AR of 1:1 and 2:1. A total of 24 shear wall racking tests was conducted. The failure modes were associated with the removal of nails from the panels, although the punching of the panels with nails also took place. It is worth noting that the nail driving schedule for walls with AR 2:1 was performed in a staggered order and the nails were driven into both double end studs instead of one to improve load transfer to the end posts since monotonic and cyclic tests of shear wall with a distance between the edges of the nails 76 mm and 50 mm and AR 1:1 showed localized failure in the form of tension in the two end studs to which the clamps were attached. All cyclic tests demonstrated localized fatigue failures of sheathing nails regardless of the type of wall. At the same time, for OSB and plywood walls, tearing and punching with nails with further damage to the panel itself was observed more than for GLG walls. This was explained by a higher density of the GLG panels compared to OSB and plywood, constituting 0.72 $g.cm^{-3}$, 0.63 $g.cm^{-3}$, and 0.48 $g.cm^{-3}$, respectively. This, in turn, prevented the breaks and slippage in the GLG panels that were observed in wood-based panels. Based on the results of studies made by Correal and Varela [89] and Varela et al. [88], it can be concluded that shear wall sheathing with GLG has similar load–displacement behaviour to shear walls sheathing with OSB and plywood panels. Shear walls with the GLG panels were affected by the edge nail spacing in the same manner as OSB and plywood. According to the results, increasing the number of nails improved the wall strength, but AR showed no effect on the peak shear strength and energy dissipation of the GLG walls. The authors recommended using adequate anchorage and force transfer details for walls with AR 1:1 and closely spaced nails due to the low capacity of the framing members. A decrease in nail spacing decreased the displacement ductility capacity and the dissipation of energy by walls, while the stiffness and maximum load-carrying capacity of the wall increased. The peak shear strength values for all panels were found to be comparable, and it is worth noting that the higher density of GLG panels allowed them to dissipate more energy and save themselves from significant damages compared to OSB and plywood. The results of the shake table test showed limited damages on shear wall sheathing with GLG panels after a strong earthquake simulation. Summing up, stiffness, maximum load capacity, and ductility of bamboo-based lateral systems were significantly affected by a number of nails, nail spacing, and sheathing panel materials, while AR of the wall didn't show any impact.

Luna and Takeuchi [90] investigated the behaviour of GLG frames with K-bracing and stiffened with GLG panels under lateral load (Fig. 6). According to load–displacement curves obtained from the tests, frames with K-bracing exhibited elastoplastic behaviour, while the elastic behaviour of frames with panels was divided into two zones such as accommodation of frames and elastic region. Both structures showed that the frames had great ductility. The maximum lateral drift allowed in Colombia by the earthquake-resistant building code is 1%, the value for which, the two types of structures tested were still in the elastic behaviour area.

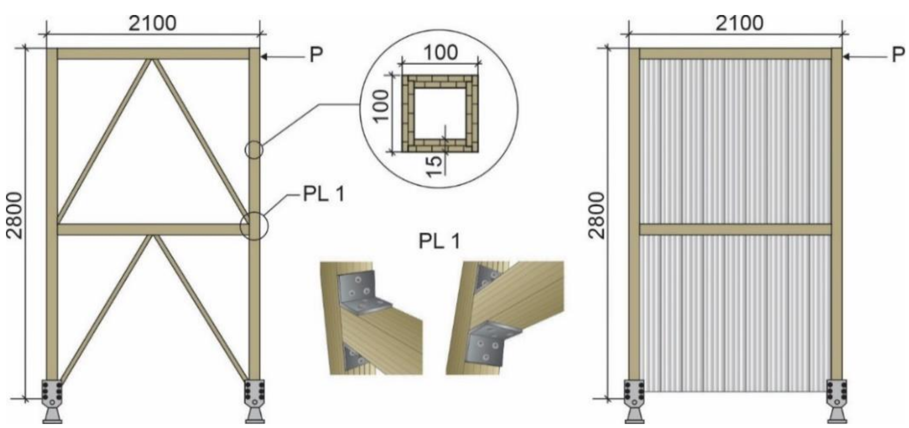

(a) (b)

Figure 6: Composition of GLG frames: a) frames with K-bracing; b) frames with panels [90]

The reviewed connections were subjected to monotonic and cyclic loads. Regardless of size, the number of nails and edge distance, the connection exhibited similar behaviour. The typical hysteretic curves for bamboo sheathing-to-framing connections were practically similar to those made of OSB and plywood. As can be seen from Fig. 7 a, the typical hysteretic loops of sheathing-to-framing connections made of bamboo were characterized by pinched unloading response [80,82,83]. The initial loading stiffness was similar to that of monotonic tests (Fig. 7 b) [82]. With an increase in displacement between cycles in the reloading phase, the reduction of the elastic stiffness and ultimate load was observed and constituted half of those in the loading condition [80,82,83].

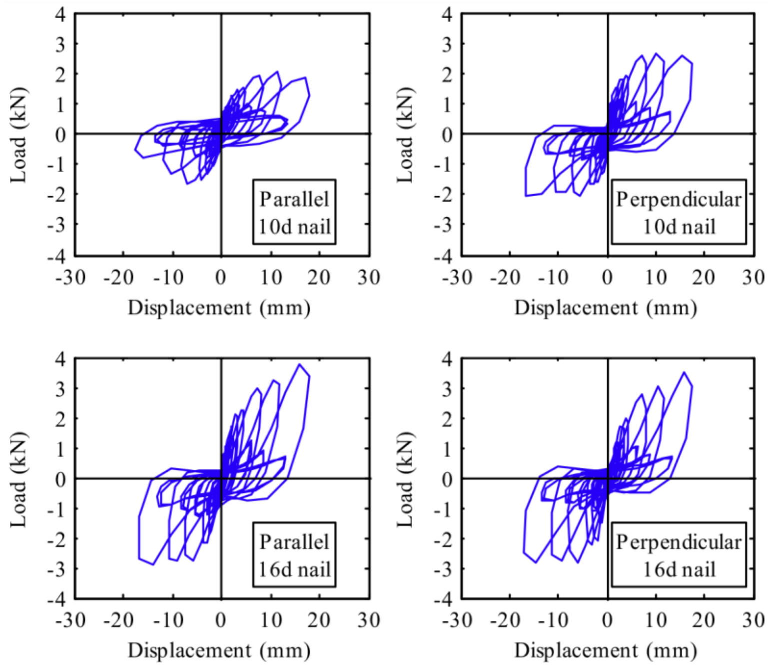

(a)

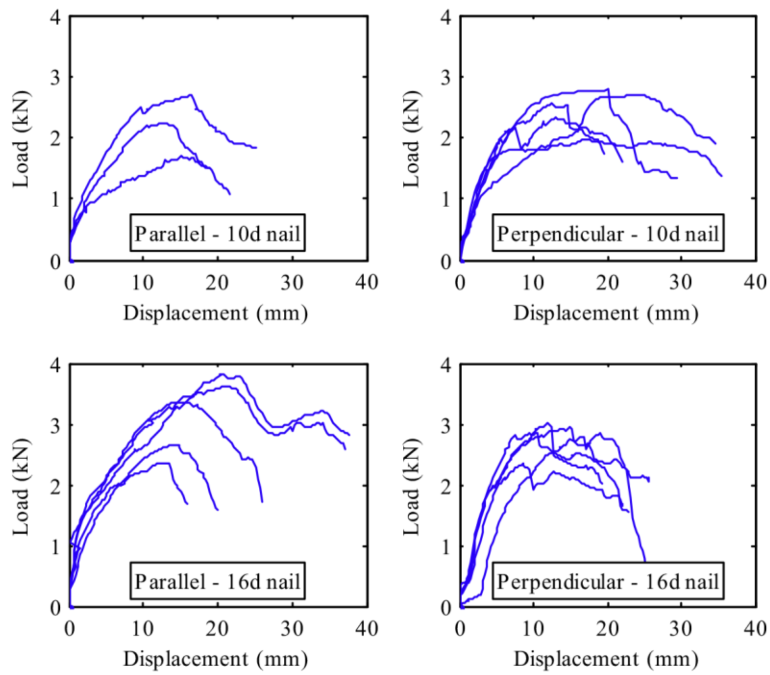

(b)

Figure 7: Typical cyclic and monotonic curves for bamboo sheathing-to-framing connections: (a) cyclic load-displacement curves; (b) monotonic load-displacement curves (taken with permission from Echeverry and Correal [83]).

The typical backbone curves observed from the cyclic test showed similar general behaviour as positive curves from the monotonic test and were characterized by the high nonlinear response when the peak load was reached [80,82] (Fig. 7 b). The connection capacity also decreased by 50–80% of the peak load in the reverse direction. It was observed, that full-scale shear walls exhibited similar behaviour, which can be explained by the mechanical properties of used nails [82,91].

2.2 Dowel-type connections

Many studies have been done to understand the behaviour of the LBL dowel-type connections and determine factors affecting their stability and strength. Table 4 provides a summary of selected papers on the mechanical behaviour of the LBL dowel-type connections.

Table 4: Selected data on LBL dowel-type connections

Species	Size, mm	Direction	Dowel type	D, mm	Standard	Sampling number	COV, %
Moso [92]	20 – 40×90×168 70 – 110×30×168	Radial Tangential	Steel dowel	9.92, 11.86, 13.95, 15.75	ASTM D 5764	3	2–16
Moso [93]	30×90×168	Radial Tangential	Steel dowel	12	ASTM D 5764	5	3–15
Moso [94]	38×50×50	Radial	Groove	6, 8, 10, 12	ASTM D 5764	12	15–30
Moso [94]	60×80×170 30×80×170	Radial	LBL dowel	6, 8, 10, 12	ASTM D5652	5	-
Guadua [95]	20.2 – 30.2×40×50	Radial Tangential Longitudinal	Wire nail	3.05, 3.76, 4.19	ASTM D 5764	5–6	8–23
Guadua [95]	20.2 – 30.2×40×50	Radial Tangential Longitudinal	Threaded bars	12.7, 19.1, 25.4	ASTM D 5764	4–5	3–22
Moso [96]	-	Tangential	Steel bolt	15.9	ASTM D 5764	15	-
Moso [97]	38×72×350	Radial	Steel dowel	12	EN 383	10	-
Moso [98]	20×40×50 40×40×50	-	Wire nail	2.5	ASTM D 5764	5–8	-
Moso [99]	20×40×150 40×40×150	-	Wire nail	2.1, 2.5, 2.8	ASTM D 1761	5	-
Moso [100]	30 – 120×120×900	Radial	Dowel	10, 12, 14, 16	ASTM D 5652	30	-
Moso [101]	30×120×250	-	Bolt	8, 10, 12, 14, 16	ASTM D 5764	3	11.84
Moso [102]	Beams 100×250×900 Columns180×250×1000	-	Bolt	14, 18, I-, L-, T-shapes	ASTM D 1761	13	-
Guadua [103]	200×300×2440	-	Bolt	10	-	3	-

According to the literature, most of the tests on the dowel-bearing strength of LBL connections were conducted based on the ASTM D5764 standard [104], which suggests two types of test configurations – half-hole and full-hole (Fig. 8).

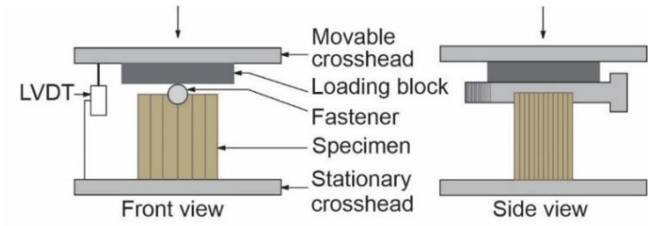

(a)

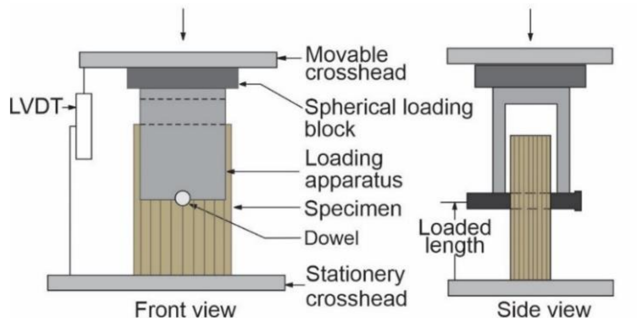

(b)

Figure 8: Configuration of tests: a) half-hole test; b) full-hole test

Cui et al. [92] conducted a full-hole test on the dowel-bearing capacity of LBL parallel to grain considering the impact of specimen size, the loaded length, and the bamboo strip arrangements. A total of 13 groups were adopted for the tests, each group has been repeated 3 times. The COV of obtained dowel-bearing properties ranged between 2 and 16%. There were 2 failure modes: crushing of fibres under the dowel hole and propagating of 1–2 shear cracks at the edge of the hole or internal buckling and peeling with light cracks (Fig. 9 a,b). According to the results, the strip arrangements had no significant effect, while with an increase in thickness and loading length, the embedding strength of the LBL connection decreased.

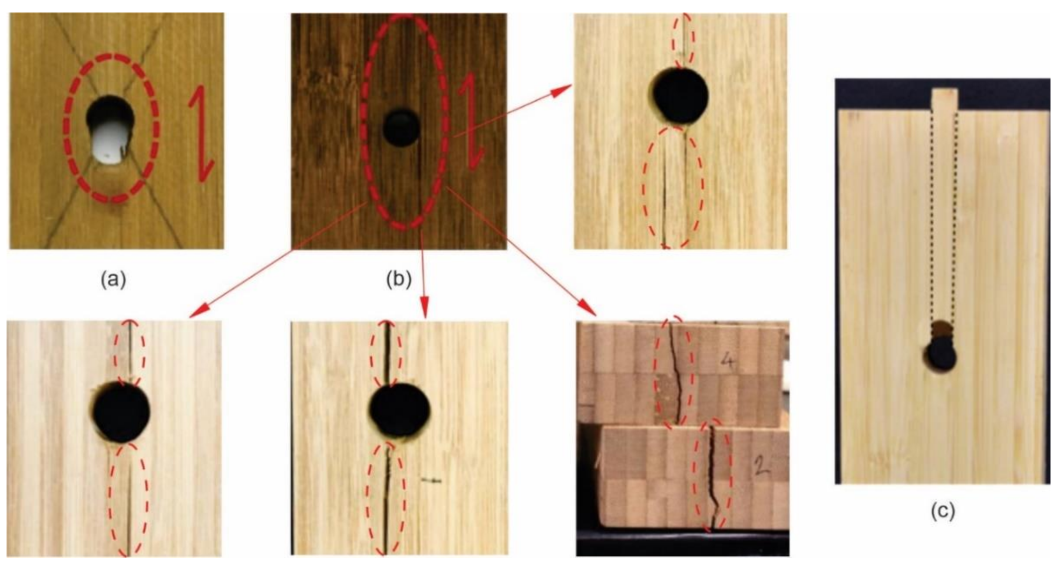

Figure 9: Failure modes of specimens parallel to grain: a) Mode 1; b) Mode 2; c) Mode 3 (reproduced from Cui et al. [93] and Reynolds et al.[97])

In the next investigation, Cui et al. [93] studied the behaviour of dowelled connections of LBL under elevated temperatures from 20˚C to 250˚C. Two types of grain directions of the laminated bamboo were studied, perpendicular to grain and parallel to grain. The target temperatures were 20˚C, 50˚C, 80˚C, 100˚C, 120˚C, 150˚C, 180˚C, 200˚C, 220˚C, and 250˚C, each test was repeated 5 times. The COV of mechanical parameters parallel and perpendicular to grain ranged between about 3–6% and 3–15%, respectively. The specimens parallel to grain exhibited 2 failure modes characterized by the fibre crushing beneath the dowel hole without a visible crack in the range of 20˚C–180˚C, and the appearance of 1–2 shear-splitting cracks on the hole edge. The specimens perpendicular to gain showed expansion of 2 cracks at an angle of 45˚along the loading direction with bamboo fibres crushing under tensile and shear stresses, and shear fracture parallel to grain from one side of the dowel to the other with densification beneath the dowel caused by compression in the range of 20˚C–100˚C (Fig. 10).

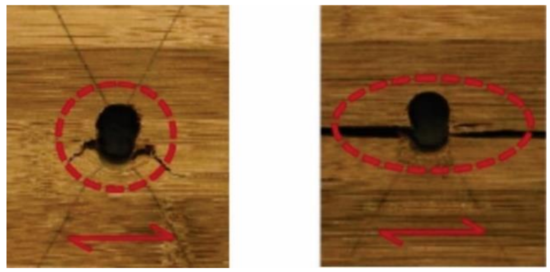

(a) (b)

Figure 10: Failure modes of specimens perpendicular to grain: a) Mode 1; b) Mode 2 (reproduced from Cui et al. [93])

All the specimens showed brittle failure regardless of the increase in temperature. The load–displacement curves for the parallel direction remained linear and reached the yielding phase after the proportional limit and showed the long plastic displacement before failure in the temperature range of 20˚C–180˚C. The curves of transverse specimens kept growing after the yielding phase, showing plastic displacement in the temperature range of 20˚C–250˚C. The turning points for both grain directions were 100˚C and 150˚C, where the load–displacement curves changed and the embedding strength increased.

Reynolds et al. [97] investigated the behaviour of dowelled connections of LBL treated by caramelization and bleaching. The test procedure was based on EN 383 [105], 10 specimens for each type of LBL were adopted. According to the results, the ductility of bleached bamboo was twice of the caramelized one. In addition to the failure modes 1 and 2 mentioned in previous studies, LBL also failed by shear plug formation (Fig. 9 c). Khoshbakht et al. [96] tested 15 replications of the LBL dowel connection as determined by ASTM D2915 [106] and gave a better understanding of the failure mechanism by finite element modelling (FEM). No glue failure was observed in the specimens. According to the results, in-plane shear stress was the primary cause of LBL failure which typically occurred off-hole centre at 1/6 of the hole perimeter left or right of the centre. Tension perpendicular-to-grain appeared to be the secondary reason for failure which occurred 7.4 mm beneath the hole, at the centre of the contact region. The FEM matched the experimental results within reasonable limits of statistical variability. High sensitivity to friction forces was observed during simulations, therefore, the effect of the coefficient of friction between the steel bolt and the LBL material on the destruction of LBL should be investigated.

When comparing load–displacement diagrams, the LBL parallel to grain showed an explicit transition from linear stage to plastic followed by cracks propagation from the dowel parallel to the loading direction. At the same time, caramelized bamboo exhibited brittle behaviour and short plastic region before fracture, compared to bleached bamboo (Fig. 11 a, b). To compare, Sitka spruce had a weakly expressed transition to a lower-stiffness plastic region (Fig. 11 c). The specimens loaded in a perpendicular direction showed a steady increase after reaching the yielding stage, the failure occurred suddenly and the load decreased quickly (Fig. 11 d).

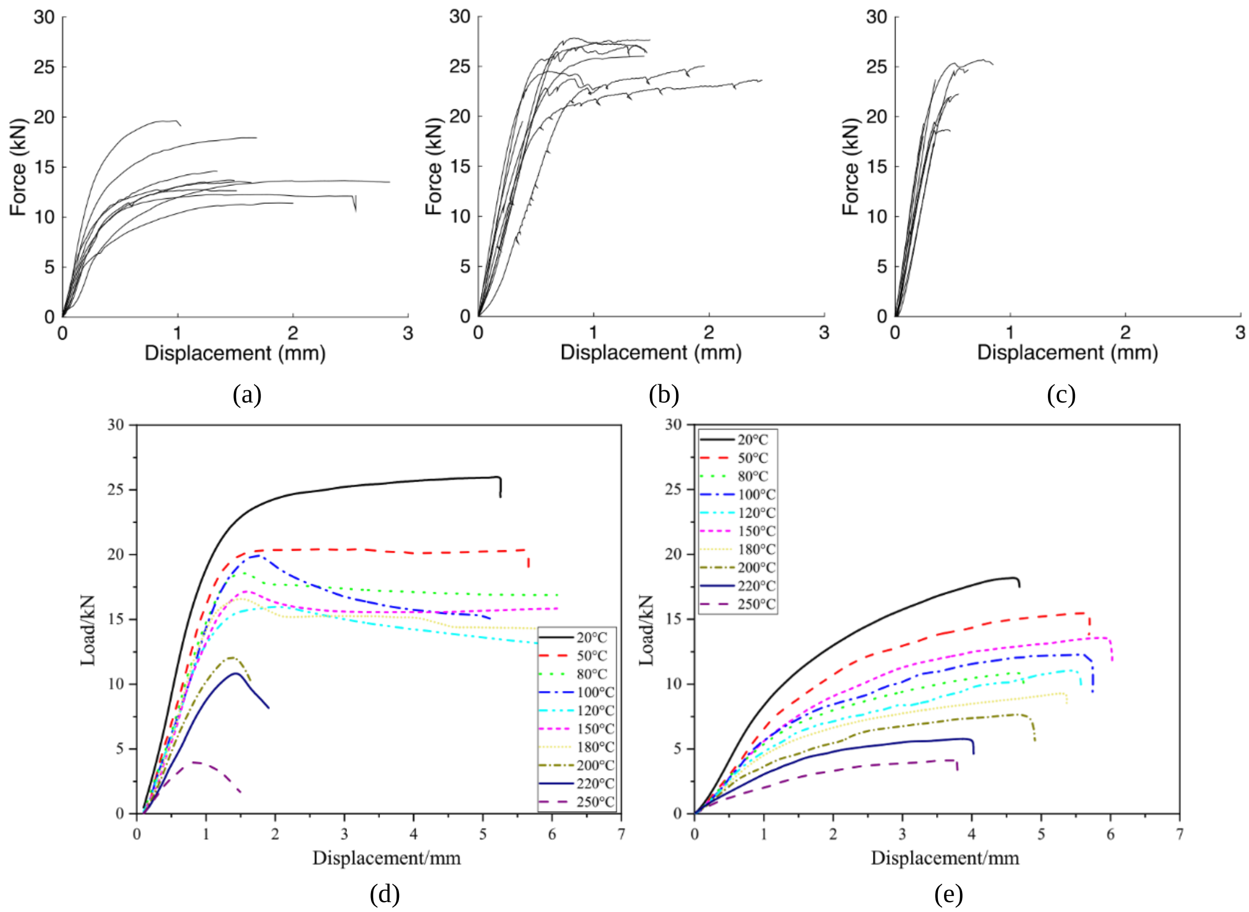

Figure 11: Load-displacement graphs: a) Sitka spruce parallel to grain; b) bleached LBL parallel to grain; c) caramelized LBL parallel to grain; d) LBL parallel to grain under elevated temperature; e) LBL perpendicular to grain under elevated temperature (taken with permission from Reynolds et al. [91] and Cui et al. [87])

Li and Zhou [94] conducted a half-hole embedment test of LBL connection according to ASTM D5764 [104], and 12 specimens for each dowel diameter (6, 8, 10, and 12 mm) were considered. Similar to fullhole test specimens, a brittle behaviour, crushing failure around the pressure head, and splitting along the fibre grain of the specimens were observed. In general, the COV from embedment tests ranged from 15 to 30% and in some cases exceeded 30%. According to Ramirez et al. [95], the dowel-bearing strength of the LBL connection depended on the diameter of the nail and threaded bar fastener and the specimen width-to-diameter ratio, since with an increase in the diameter the dowel-bearing strength decreased due to the volume effect under the fastener hole. The dowel-bearing strength of the LBL connection was higher in the parallel direction than in the perpendicular direction. The authors compared the behavior of LBL connections considering embedding load directions (longitudinal, tangential, and radial), 45 and 115 tests were conducted on groups of nails and threaded bars, respectively. Each group contained from 3 to 6 specimens. The results showed that tangential and radial directions were similar and could follow the same design rules. Curves for loading parallel to the grain showed a linear increase up to the LBL bearing yielding (5% offset), and the stresses remain almost constant beyond this point. Curves for loading perpendicular to the grain showed a linear increase up to the LBL bearing yielding, followed by a continuous stress increase until the end of the tests. The COV values of bearing strength for each dowel diameter and load case were in the range of 3 and 23% which complies with the general experience mentioned in ASTM D5764 [104]. The authors developed a three-dimensional FEM and determined the depth of the bearing zone which depended on the fastener diameter of 1.6D, and local material properties under the fastener which were obtained as a function of the LBL bulk properties. The expressions for calculating the LBL dowel-bearing strength as a function of the fastener diameter and the specimen width-to-fastener diameter ratio were presented, however, they were valid only for the range of diameters considered in the study. Li and Zhou [94] investigated the load-carrying capacity of the LBL connection under lateral load according to ASTM D5652 [107]. The test dowel diameters were 6, 8, 10, and 12 mm, 5 specimens were adopted for each group. The specimen was made of the main member and side members assembled by the LBL dowel and there was no adhesive on the interface. According to the results, the failure mode of the connection test under lateral load was the dowel yielding with two plastic hinges which was similar to Mode IV of the European Yielding Model (EYM) [94] (Fig. 12).

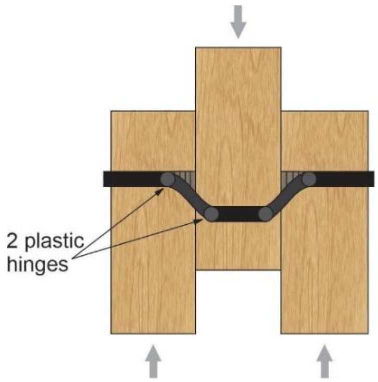

Figure 12: The failure Mode IV of the LBL connection under lateral load

Chen et al. [98] investigated the LBL-to-LBL connection consisting of LBL main member nailed between two LBL plates (Fig. 13).

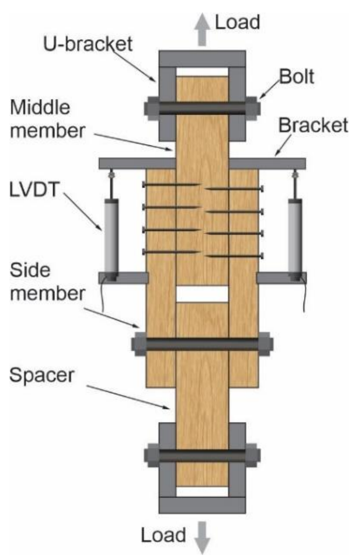

Figure 13: Test setup for nailed joints (reproduced from Chen et al. [98])

The test procedure followed the ASTM D1761 standard [84], 23 groups of nailed LBL joints were tested under monotonic loads, with 5–8 replicates tested for each series. According to the results, the connection had three failure mo3des characterized by bearing failure, splitting failure, and row shear failure. To prevent brittle failure in nailed connections, the authors provided limiting ranges for end distance, edge distance, row spacing, and centre-to-centre spacing as 6D, 2–3D, 3D, and 6D, respectively. With an increase in centre-to-centre and end distances, the capacity of nailed joints also increased until the spacing was exceeded. Chen, Yang [99] conducted push-out tests to study the effect of nail arrangements on the strength, stiffness characteristics and load-displacement response of LBL nailed connections (Fig. 14).

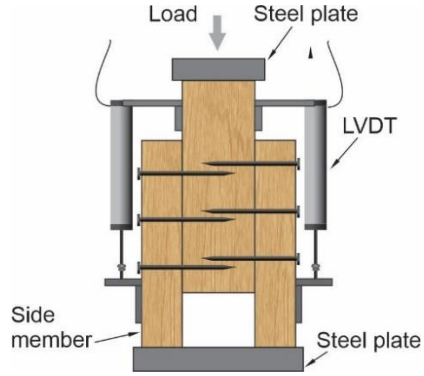

Figure 14: Test setup for nailed joints (reproduced from Chen et al. [99])

A total of 125 specimens were tested, with 5 replicates for each group: nail diameter (2.1, 2.5, and 2.8 mm), number of nail rows (1, 2, and 3), and number of nail lines (1, 2, 3, 4 and 5). The tests were conducted following the requirements of ASTM D1761 [84]. According to the results, the arrangement of nails has a significant impact on failure modes. Both embedding and splitting failures were observed in LBL nailed connections. An increase in the diameter and number of nails in a row led to a better capacity of connections and lower ductility.

Cui et al. [100] studied the behaviour of steel-to-laminated bamboo dowel connections with a slotted-in steel plate under tension based on the ASTM D5652 [107] (Fig. 15), 4 groups were prepared corresponding to the end distances of the connections (5D, 6D, 7D, and 8D), each test was repeated 3 times. All the dowels showed 3 types of failure modes described in the EYM (Fig. 16).

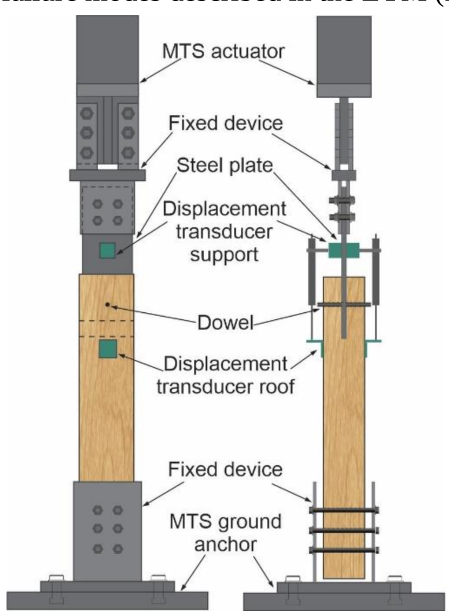

Figure 15: Test setup for steel-to-laminated bamboo dowel connections with a slotted-in steel plate: a) front view; b) lateral view (reproduced from Cui et al. [100])

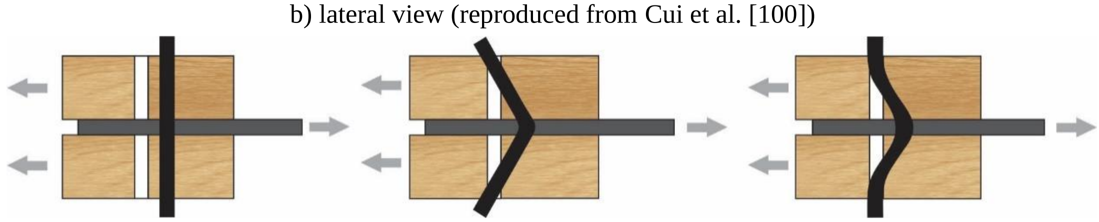

(a) (b) (c)

Figure 16: The yield modes of dowel-type fasteners in timber connections: a) Mode I; b) Mode II; c) Mode III

Mode I was characterized by the crushing of wood fibres under the dowel, no fasteners bending and through cracks were observed. This type of failure happened when the thickness of the side members and the thickness-to-diameter ratio were small while the bending strength of the dowel was big and the shear strength parallel to grain of LBL was low. In Mode II, fasteners were deformed in bending at one plastic hinge point per shear plane, with a predominant bearing yield of wood fibres in contact with the fasteners in side members. In Mode III, wood fibres locally crushed near the shear planes with fasteners yield in bending at two plastic hinge points per shear plane. Mode III occurred in specimens, where the thickness-to-diameter ratio was large enough because the bearing zones became larger and dowel bending was restrained. The connection members mainly failed in shear or splitting failure, while the dowel showed the one-hinge yield mode (Mode II).

The yield, ultimate load, and initial stiffness significantly increased and the ductility ratio decreased with an increase in the diameter from 10 mm to 16 mm. It should be noted that the bearing area between the dowel and bamboo material was defined by the dowel diameter and its increase could change the failure mode of the connection from embedding or splitting failure to shear failure. According to the results, the change in thickness didn't affect yield load but a decrease in the thickness of the dowel diameter led to a larger load-carrying capacity. Various end distances insignificantly affected the yield load. Specimens with an end distance of 6D–8D exhibited better ductility and embedding failure.

In the connections with the LBL dowel, the load-displacement curves were in the linear elastic stage before brittle failure occurred in a sudden manner [94]. To compare, the LBL nailed connections exhibited similar load-slip responses regardless of the number and arrangement of nails [99, 101]. The brittle failure of LBL nailed connections was characterized by the elastic stage, nonlinear stage, and descending stage (Fig. 17).

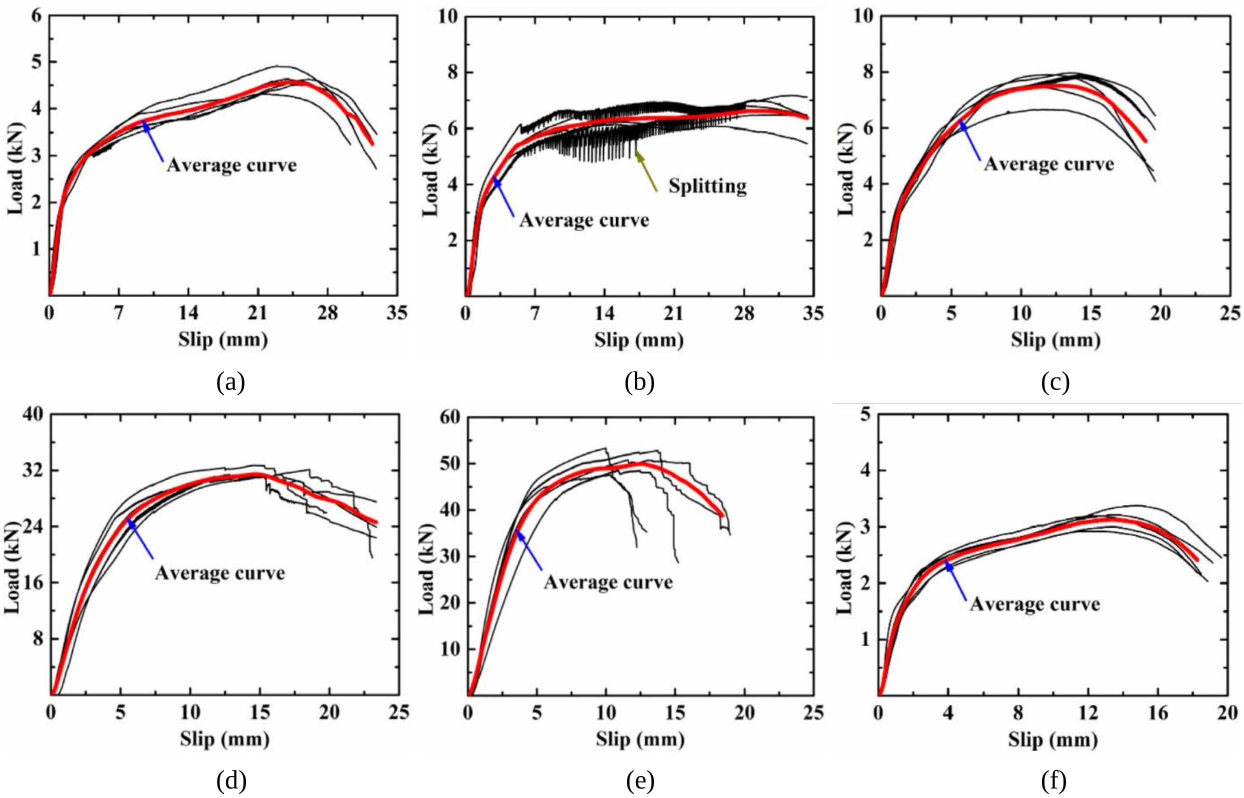

Figure 17: Typical load-slip response of LBL nailed connection: a) 2.1-R1L1; b) 2.5-R1L1; c) 2.8-R1L1; d) 2.1-R1L3; e) 2.5-R3L3; f) 2.5-R3L5 (taken with permission from Chen et al. [99])

At the beginning of loading, the load displayed linear characteristics with the increase in the relative slip between the side and main members, and then a nonlinear increase until the ultimate load was reached.

Before the failure was reached, the splits which occurred in the members, led to sporadic decreases in load in most specimens. Afterwards, the load started to decline very slowly up to the final failure, representing the occurrence of splits in the middle or side members. Nevertheless, the specimens didn't completely lose the capacity of withstanding load.

Similar to the LBL nailed connections, the typical load-displacement curves of steel-to-laminated bamboo dowel connections with a slotted-in steel plate under tension were also divided into a linear stage, a nonlinear stage within and beyond the proportional limit, and descending stage.

2.3 Bolted connections

Leng et al. [102] compared the moment-rotation behaviour of 3 types of LBL beam-to-column connections: 1) conventional bolted connections with clotted-in steel plates (I-connection), 2) T-shaped extended end plate connections with side plates that confine the beam, 3) L-shaped end bracket connection which partially confines both the beam and column (Fig. 18).

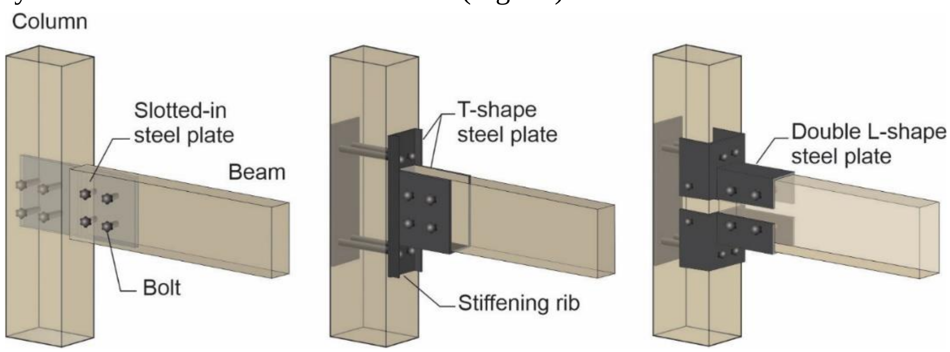

(a) (b) (c)

Figure 18: Three types of bolted beam-to-column connections: a) bolted connections with slotted-in steel plates (I-connection); b) bolted connections encased with T-shape steel plates (T-connection); c) bolted connections encased with double L-shape steel plates (double L-connection) (reproduced from Leng et al. [102])

A total of 13 specimens were adopted for tests (7 monotonic, 6 cyclic). A monotonic test was carried out following ASTM D1761 [84] and cyclic test – Test Method B of ASTM E2126 [108]. According to the results, failure of the specimens under monotonic and cyclic loads was characterized by brittle behaviour and caused by splitting parallel to grain direction, which started at the bolt line. However, the monotonic specimens with the cross-laminated arrangement in the connection region failed due to delamination between laminas, and the splitting was effectively reduced. Based on test results, T- and L-connections increased elastic stiffness, plastic stiffness, load-carrying capacity, and ductility by 215% and 169%, 153% and 53%, 58% and 50%, 15%, and 13% compared to I-connections, respectively. For T-connections, the influence of bolt arrangement was negligible compared to I-connections, which showed a lower elastic stiffness when more bolts with smaller diameters were used. The authors stated, that EC5 conservatively estimated the bearing capacities of the T- and L-connections. For the I-connections, the safety margin was significantly smaller.

Castaneda and Bjarnadottir [103] concluded, that improving the stiffness is of great importance in the design of the I-shaped beam. The author tested three different configurations of bolted connections to create an optimal composite bamboo I-shaped beam which was stiffer and safer in structural applications. The configurations were: beam bolted at each support and midspan with steel angle at the bolts (B1), beam bolted at each support and quarter points along the full span of the beam with steel angle at the bolts (B2), and beam bolted at each support and every 30.5 cm across the full span of the beam with steel angle along the entire span of the beam (B3). The authors developed a three-dimensional model based on the bilinear stress-strain relationship, shear modulus of elasticity determined by the model of Saliklis and Falk [109], and orthotropic behaviours of the beam obtained from experimental results with transversal isotropic in the radial-tangential plane [95]. According to the results, B3 was the most optimal configuration of bolts since deflection and maximum stress concentration were reduced by 48% and 72% compared to B1 and B2, respectively. In addition, better contact between bodies was observed in B3 which led to a stiffer I-shaped beam. To compare, B1 had the highest maximum stress concentration and deflection, while B2 showed a slight improvement over B1.

Tang et al. [101] investigated the behaviour of single-bolted and multiple-bolted connections using LBL and steel plates (Fig. 19).

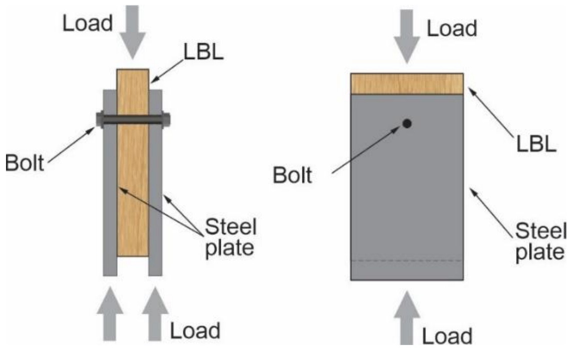

(a)

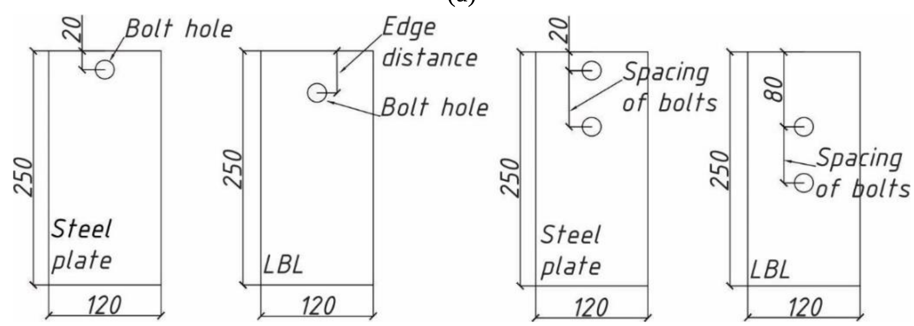

(b)

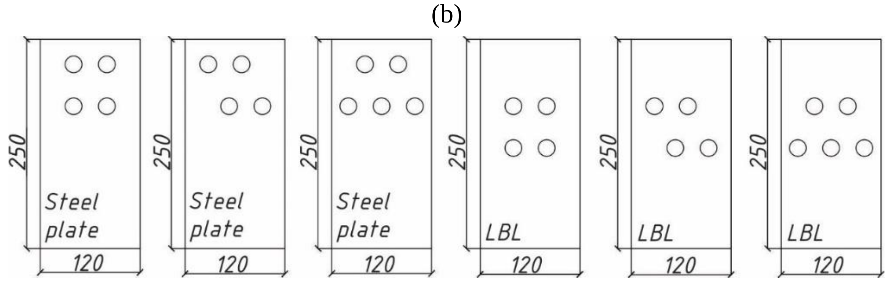

(c)

Figure 19: Test setup for single-bolted and multiple-bolted connection: a) profile and front view of single-bolted joint; b) dimensions of single-bolted and double-bolted joints; c) dimensions of multiple-bolted joints; (reproduced from Tang et al. [101])

A total of 14 groups of bolted LBL connections with 3 specimens for each group (edge distance, bamboo thickness, and bolt size) were tested with reference to the bolted connection tests on timber and bamboo in the literature. The variations of load-carrying capacities for single-bolted connections were within 11.81%. Meanwhile, the COV values of load-carrying capacities of multiple-bolted connections were within 9%, showing good consistency. For both single-bolted and multiple-bolted connections, the failure modes were characterized by longitudinal splitting, shear out, and combined longitudinal splitting and bamboo crushing (Fig. 20).

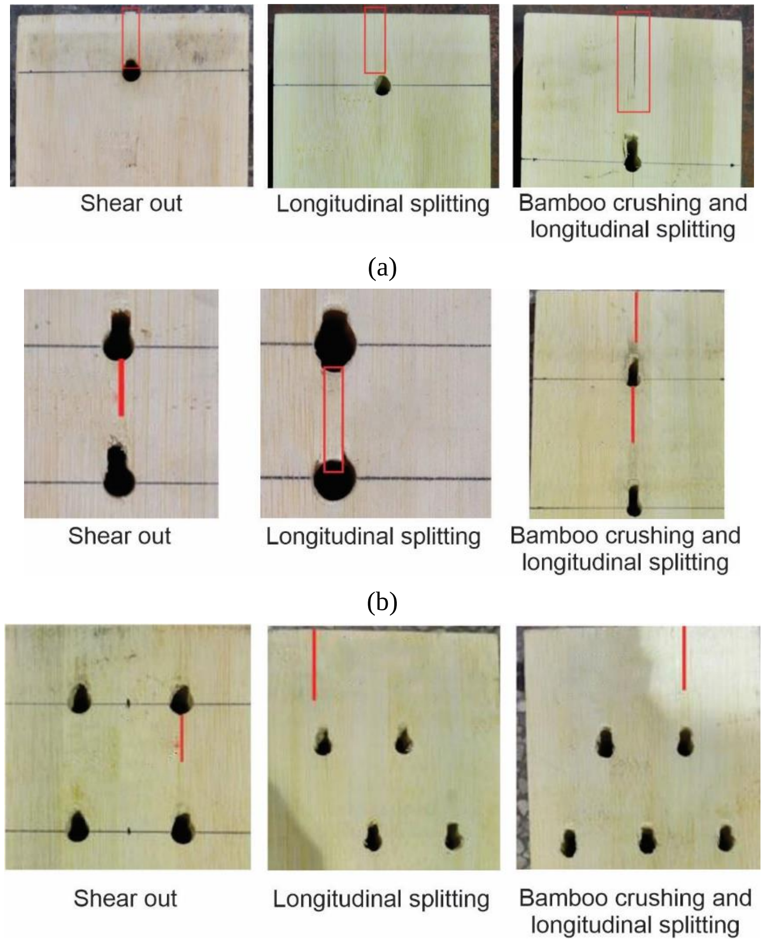

(c)

Figure 20: Failure modes of single-bolted and multiple-bolted connection: a) single-bolted; b) two-bolted; c) multiple-bolted connection (reproduced from Tang et al. [101])

For single-bolted connections, the capacity increased with an increase in bolted diameter and edge distance. When the edge distance in a single-bolted connection and the spacing in a multiple-bolted connection were bigger than 5D, the connection capacity was stable. In addition, the stagger arrangement of the bolts led to a better capacity of multiple-bolted joints. The authors established parameters of the constitutive relation and Hill's failure criterion and used them for computational models of the connection. The computational results were in good agreement with the test results. ASTM D5764–97a used for timber connection appeared to be unsuitable for strength prediction of the bolted LBL connections.

2.4 Glued-in rods (GIROD) connections

Glued-in rod (GIROD) connection is one of the most promising and highly effective methods of connection that are currently being investigated and used in wood and bamboo engineering. Typically, GIROD consists of one or more rods glued to solid wood or wood- and bamboo-based construction material. Over the past decade, an extensive study of GIROD in timber has been conducted [110-117]. There are few investigations on GIROD-LBL connections in the existing literature. Yan et al. [118] carried out both-ends pullout test on GIROD-LBL (Fig. 21) according to ASTM D1761–88 [119], 8 samples were adopted for each group corresponding to rod diameter (8, 12 am 16 mm) and rod embedded depth (40, 80, 120 and 160 mm). The specimens showed 2 failure modes, which were threaded rod rupture and adhesive interface failure. According to the results, an increase in the diameter and depth of the threaded rods increased the pullout peak load of both-end GIROD-LBL. The normal shear strength of threaded rods glued-in LBL was governed by interfacial shear strength between glue and base materials, so increasing the contacting area was suggested to improve the strength of the connection. The authors suggested using 4.8 rods with a slenderness ratio of 10 or over to satisfy interface stability and a tensile load of the metal used in the connections.

Figure 21: GIROD-LBL connection specimen (reproduced from Yan et al. [118])

Zhang et al. [120] evaluated the pull-out capacity of threaded steel glued with two-component epoxy resin into LBL under axial load. The test procedures followed ASTM D1761–88 [119], the total number of all test specimens was 125 considering the edge distances, the glue thicknesses, the rod diameters, and the slenderness ratios. The COV values of the obtained failure loads were within 10%. Similar to previous studies, the anchorage length and rod diameters affected the failure load, which increased with an increase in the slenderness ratio until the critical value was achieved. Based on the analysis of variance, the effects of glue thickness, edge distances, and rod diameters were statistically significant since the corresponding p-values were less than 0.05. To avoid splitting behaviour and ensure better load-carrying capacity, the edge distance should be more than 3D and the thickness of a glue line should be 2 mm. The shear failure at the bamboo and adhesive interface was the main failure mode, therefore the interfacial shear stress between these layers determined the normal shear stress (Fig. 22).

Figure 22: Typical GIROD-LBL failure modes (extracted from Zhang et al. [120])

The authors compared several design equations and models established for GIROD-wood connections and concluded that the Riberholt design equation [121] was consistent with the experimental test results, the EC5 [122] and Feligioni design methods [123] predicted unreliable estimates, whereas the DIN 1052 [124] design equation showed conservative results.

3 Numerical models

3.1 Numerical models for sheathing-to-framing connections

Several attempts have been done to describe the load-displacement relationship and predict the yield strength and bearing capacity of bamboo-based sheathing-to-framing connections (Table 5).

Table 5: Numerical models for LBL sheathing-to-framing connections

Model	Equation	Predicted parameter	Error, %
NDS [83]	$Z=\frac{k_3 D l_s F_{em}}{\left(2+R_e\right)R_d}$ $k_3=-1+\sqrt{\frac{2\left(1+R_e\right)}{R_e}+\frac{2F_{yb}\left(2+R_e\right)D^2}{3F_{em}l_s^2}}$ $R_e=F_{em}/F_{es}$	Yield Strength	28-30
EYM [82]	$F_{fR}=f_{h.t}db_1+F_{\alpha\chi,R}\frac{10\left(b_1+b_2\right)+0.5\left(b_1+b_2\right)^2}{100+\left(b_1+b_2\right)^2}\cdot\frac{l-t_2-b_1}{l-t_2}$ $f_{h,b}=\frac{1}{86}\rho^{1.331}d^{-0.257}$ $F_{\alpha\chi,R}=54.12\cdot L\cdot d\cdot S_G^{2.5}$	Bearing capacity	15
Echeverry and Correal [83]	Governing equations can be found in [120]	Bearing capacity	N/a
Echeverry and Correal [83]	Governing equations can be found in [120]	Load–displacement relationship	N/a
Modified Foschi model [80]	$P=\begin{cases}\left(P_0+K_2\Delta\right)\left(1-\exp\left(-\frac{k_0\Delta}{P_0}\right)\right), if\ \Delta\le\Delta_{peak}\\ P_{peak}+K_3\left(\Delta-\Delta_{peak}\right), if\ \Delta_{peak}<\Delta\le\Delta_{fail}\end{cases}$	Load–displacement relationship	22.02-34.41

Note: Z – reference lateral design value; D – diameter of the dowel, in (see NDS Table 12.3.7 [87]); l_s – side member dowel bearing strength, in; F_{em} – main member dowel bearing strength, psi (see NDS Table 12.3.3 [87]); F_{es} – main member dowel bearing strength, psi (see NDS Table 12.3.3 [121]); R_d – reduction term (see NDS Table 12.3.1B [87]); F_{yb} – dowel bending yield strength, psi; F_{fR} – bearing capacity of timber-bamboo connectors; $f_{h,b}$ – embedment strength, MPa; ρ – wood or bamboo material density, kg/m^3; d – diameter of the nail, mm; $F_{ax,R}$ – nail withdrawal capacity; L – the penetration depth; S_G – specific gravity of wood or bamboo materials; P_{peak} – peak load, N; Δ_{peak} – corresponding displacement of peak load, mm; Pu – ultimate load, N; Δ_u – ultimate displacement, mm.

As can be seen, American code NDS used by Sinha et al. [81] overestimated the yield strength of LBL sheathing-to-framing connections, and the relative difference between experimental and predicted results constituted 28–30%. The EYM model used by Li et al. [82] relatively accurately predicted the bearing capacity of the connections, with an error lower than 15%. Echeverry and Correal [83] developed a numerical model in the software CASHEW to obtain the typical load-displacement response and cyclic behaviour of LGM shear walls (Fig. 23).

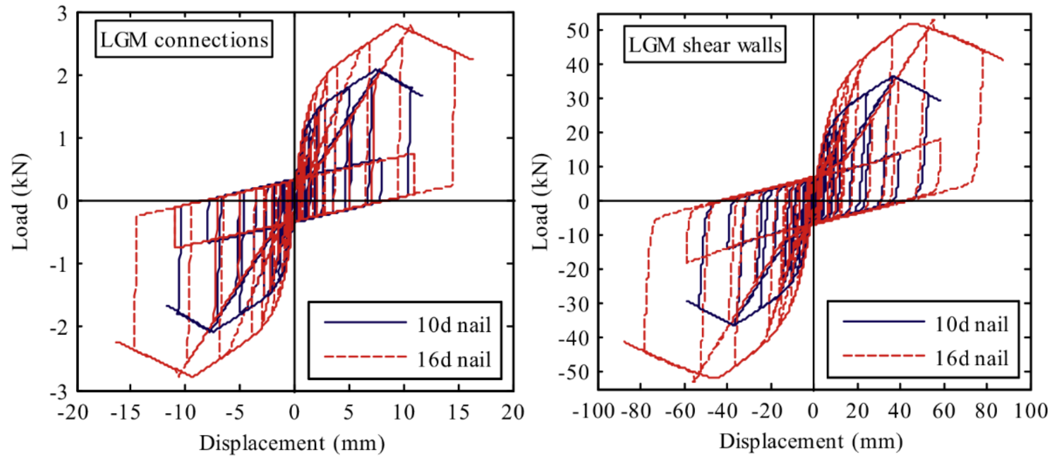

Figure 23: Typical models of load-displacement relationship and cyclic behaviour of LGM shear walls: a) load-displacement response model; b) estimated cyclic behaviour (taken with permission from Echeverry and Correal [83])

The model provided a preliminary comparison with wood-framed shear walls, showing that bamboo-based shear walls can be an alternative to conventional wood-framed construction, considering the similar shear capacities expected. Sun et al. [80] proposed the exponential prediction equation to describe the shape of the load-displacement curves. As can be seen, the difference between tested and fitted values constituted up to 34.41%, calling for further research for a complete experimental characterization of bamboo-based shear wall behaviour, considering a wider range of nail diameters and sample sizes.

3.2 Numerical models for dowel-type connections

The design rules from Europe, the United States, Canada, and China, including EC5 [126], NDS [87], CSA O86 [127], and GB 50005 [128], were collected and proposed by scholars to predict the load-carrying capacity, embedment strength and the effective number of nails of bamboo-based dowel-type connections. Fig. 24 shows the accuracy of predicted load-carrying capacity using existing calculation models.

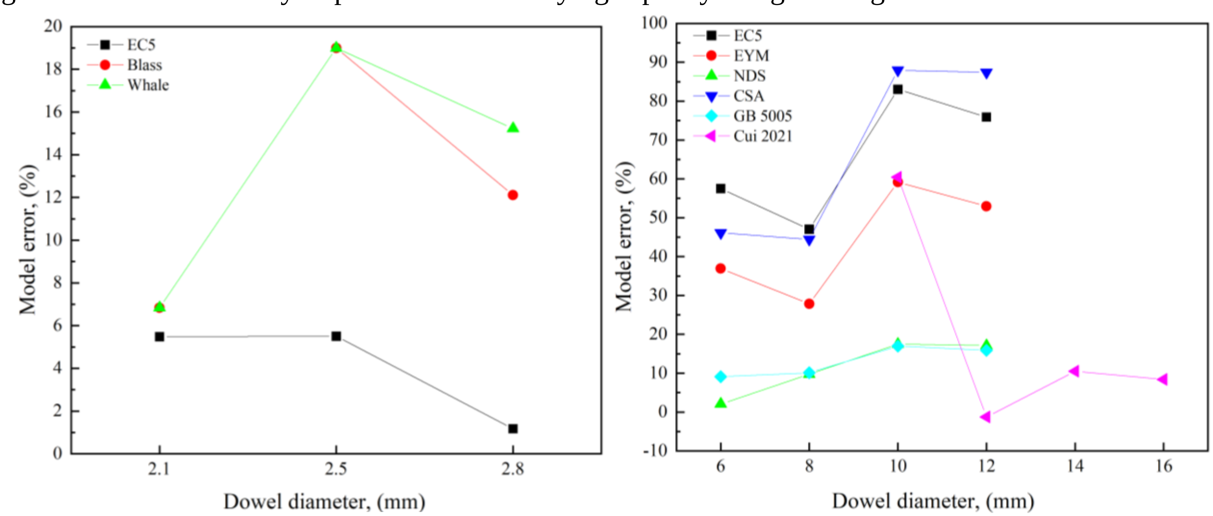

(a) (b)

Figure 24: Error analysis of the load-carrying capacity of LBL connections: a) smaller dowel diameters; b) bigger dowel diameters (data is taken from the reviewed literature in Table 4)

According to errors analysis, the EYM established in EC5 can accurately predict the capacity of the LBL nailed connections with smaller diameters (Fig. 24 a). It was found that the relative difference between the experimental and calculated values by Blass et al. [99] and Whale et al.[99] increased with the increase in the diameter of nails. Fig. 24 b shows, that EC5, EYM, and CSA showed conservative results for bigger dowel diameters with a relative difference of 20–90%. Among national standards, the results calculated with NDS and GB5005 were the closest to experimental results; and the relative difference was less than 15%. Cui et al. [100] proposed a set of equations to predict the behaviour of the steel-to-laminated bamboo dowel connection with a slotted-in steel plate. Although the predicted failure modes were accurate, the calculated results were conservative. The authors introduced the modified coefficient C_g to accurately predict the load-carrying capacity of the connections. However, considering the limited number of connections, the modified coefficient suggested in the paper needs to be further verified. Table 6 shows the governing equations of proposed models with better accuracy for calculating the load-carrying capacity of LBL dowel-type connections.

Table 6: Numerical models for bearing capacity of LBL dowel-type connections

Model name	Dowel diameter, mm	Equation	Error, %
EU5 [99]	2.1–2.8	Governing equations can be found in [93]	4.05
NDS [100]	6–12	Governing equations can be found in [94]	11.61
GB5005 [100]	6–12	Governing equations can be found in [94]	13.01
Cui et al. [100]	12–16	$R=\begin{cases} f_e dt, \frac{t}{d} \le 0.66\sqrt{\frac{f_\gamma}{f_e}}, \\ f_e dt\left(\sqrt{2+\frac{0.88 f_y d^2}{f_e t^2}}-1\right), 0.66\sqrt{\frac{f_\gamma}{f_e}} \le \frac{t}{d} \le 1.88\sqrt{\frac{f_\gamma}{f_c}}, \\ 0.94d^2\sqrt{f_\gamma f_c}, \frac{t}{d} \ge 1.88\sqrt{\frac{f_\gamma}{f_e}} \end{cases}$ $f_{e,par} = \left(-0.0236D + 1.471\right) f_{c,0}$	5.89

Note: $f_{e,\,par}$ – embedding strength of the LBL parallel to grain, MPa; $f_{c,\,0}$ – compressive strength of the LBL parallel to grain, MPa; t – is the thickness of side member, mm; d – is the dowel diameter, mm.

The scholars used and compared two general methods for embedding strength of LBL connection based on compression strength, density, and dowel diameter as major influencing factors adopted in different national standards [87,126,129–132]. However, the calculated results were smaller than the experimental ones since the moisture content (MOC) of LBL was smaller than the 12% specified in some formulas, and the strength-to-weight ratio of LBL was larger than that of conventional wood materials [93].

Cui et al. [93] proposed a tri-linear model for both grain directions to evaluate the embedding strength reduction of LBL connection at elevated temperature (t), where ηT was defined as the ratio of embedding strength at elevated temperatures to that at ambient temperature, and 0.50 was used in the temperature range of 100–180˚C to simplify the calculation:

$$\eta_T = \begin{cases} -0.0063T + 1.125 & 20°C \le T \le 100°C \\ 0.50 & 100°C \le T \le 180°C \\ -0.005T + 1.400 & 180°C \le T \le 280°C \end{cases} \quad (1)$$

To calculate the embedding strength of LBL connection considering the effect of the different factors, Cui et al. [92] adopted a fitting model based on dowel diameter and compressive strength as major influencing factors expressed as:

$$f_e = \left(-0.0236D + 1.471\right) f_{c,0} R^2 = 0.8935 \quad (2)$$

The parameter ranges of $2D \leq T \leq 3D,\ H = 7D,\ 6D \leq B \leq 9D$, where D, H, B are the dowel diameter, loading length, and thickness of the specimen in mm, $f_{c,0}$ is the compressive strength in MPa. The calculating results were in good agreement with the experimental results.

Many countries evaluate the load-carrying capacity of the entire connection by multiplying the capacity of a single nail by the effective number of nails, and the calculated results appeared to be higher than the actual results obtained from the experiment [99]. According to previous studies on timber, this happens due to unequal distribution of loads in a connection with multiple fasteners, and due to failure of the first and last fasteners since they receive the highest load level [133–136]. Calculation methods based on EC5, SIA 265 [132], and Jorissen [137] provided overestimated or conservative predictions of the effective number of nails in a row [98], while the formula proposed by Hossain et al. [138] can adequately predict the effective number of nails [99] (Fig. 25).

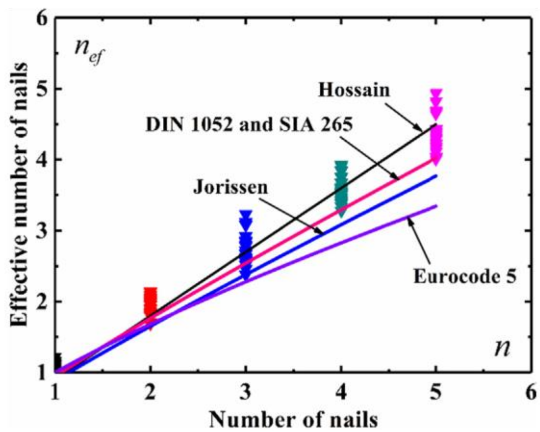

Figure 25: Effective number of nails (taken with permission from [99])

For LBL-nailed connections, Chen et al. [98] proposed the formula to predict the bearing capacity of the LBL connection with multiple nails in a row by multiplying the lateral load capacity of the single-nail joint by the effective number of nails in the row:

$$n_{ef} = \min \begin{cases} n \\ n^{0.9} \left(\dfrac{s}{6D} \right)^{0.25} \end{cases} \quad (3)$$

Where, n_{ef} is f is the effective number of nails in a row parallel to the grain, n – is the number of rows.

In addition, Foschi's formula [139] accurately described the load-slip of LBL nailed connections with different configurations [98], and Folz formula [125] was suitable for the description of the load-slip relationship of the LBL nailed connection loaded laterally [99].

4 Discussion

4.1 LBL and wooden sheathing-to-framing connections

For LBL sheathing-to-framing connections, the material type and nail spacing appeared to be the main influencing factors of load-carrying capacity. However, in wood connections, wall AR also significantly affected lateral behaviour. In general, both LBL and wood sheathing-to-framing connections shared similar behaviour. In the reviewed studies, BOSB and GLG panels were used as sheathing materials, and LBL was used as framing members. The type of nail appeared to affect the failure mechanism of the connections: for wire nails, the failure mode was characterized by nail yielding and pulling through framing member, while for self-tapping screws – by brittle failure. Edge distances also affected the failure behaviour of nails since increased edge distance led to nail withdrawal and partial nail head pulling through the framing member, while small distances caused sheathing edge-tear. At the same time, the LGM panel didn't show any nail withdrawal from the framing member or fatigue. The energy dissipation capability of the LGM panels was lower compared to that of BOSB or wood panels. This was due to the different strip configurations in the LGM panels and the presence of voids and imperfections, which in turn calls for optimization of the processing method of LGM.

Among reviewed sheathing materials, the strength and energy dissipation of BOSB and GLG were higher than those of wood and the LGM panels due to a higher density of the former which led to more bending on the sheathing nails instead of wood crushing. Therefore, steel nails could contribute more to energy dissipation on walls sheathed with bamboo panels than OSB and plywood panels where more wood crushing was observed. However, the high density of bamboo materials caused a lower ductility of the connection itself, which in turn caused earlier nail fatigue. Nonetheless, the ductility demand at 2% of the drift for GLG-sheathed walls was still comparable with the plywood and OSB-sheathed walls.

Finally, the ultimate displacement capacity of the plywood and OSB walls and their BOSB/GLG counterpart was almost the same, suggesting that bamboo walls would be able to withstand similar earthquake displacement demands than those for walls sheathed with OSB and plywood. In full-size shake table tests, shear walls and frames with GLG panels and K-bracings were subjected to a sequence of ground motions with increasing intensity that was representative of those expected in a high seismic hazard zone in Colombia, and earthquake records of El Centro (California, 1940), Quindío (Colombia, 1999), Northridge (California, 1994) and Kobe (Japan, 1994) were the selected. The structures showed slight damage, and both frames with panels and K-bracings were at the elastic stage when the maximum allowed displacement reached 1% based on Colombian standard, which allowed the frames to return to their initial condition.

4.2 Dowel-type and bolted LBL and wood connections

The studies were conducted on the embedding strength of dowel-type LBL connections. According to the results, dowel-type LBL joints exhibited three failure modes: fibres crushing beneath the dowel hole, 1–2 shear splitting cracks on the hole edge, or internal buckling and peeling with insignificant cracks, and shear plug formation. It is worth noting that there were no failures along the glue line, therefore the failures were caused by in-plane shear stress and tension perpendicular-to-grain. All dowel-type LBL connections loaded in parallel directions exhibited an elastic-plastic behaviour with a pronounced yielding phase before a constant stress increase until the end of the test or brittle failure.

Connection tests on dowel-type LBL showed three failure modes such as bearing failure, splitting failure, and row shear failure. The brittle behaviour of the LBL nailed connections included the elastic stage, nonlinear stage, and descending stage. Similar behaviour was observed in wooden joints, in which failure modes included splitting, row shear, block shear, and net tension. The yield modes of dowel-type fasteners in the LBL connections were similar to those in timber connections described in EC 5 [126].

Similar to wood, the mechanical behaviour of dowel-type and bolted connections was governed by several geometric, material, and loading parameters like material density, fastener slenderness, end and edge distances, spacing and number of fasteners, and loading configuration. However, LBL joints turned out to be stiff and brittle compared to wood connections. Dowel-type wood connections can show both ductile and brittle behaviour. Since timber is prone to brittle failure when bent and stretched, joints are the key to the ductility of timber structures. Brittle behaviour is not desirable in buildings, since sudden destruction of the structure can lead to human and material damage. Therefore, ductile behaviour is considered the most desirable, especially in areas of increased seismic hazard due to the consistent deformation of the structure, which helps to identify and eliminate possible destruction in time and ensures proper structural strength. To avoid brittle behaviour in the LBL connections, the scholars provided limiting values for end distance, edge distance, row spacing, and centre-to-centre spacing which were 6D, 2–3D, 3D, and 6D, respectively. The edge distance limits appeared to be the same for Douglas-fir and spruce [140], while the minimum end distance for wood-nailed connections loaded parallel to grain with and without pre-bored holes was 15D and 10D [141].

Many models have been developed to predict the brittle behaviour of wood connections. Taking into account the similarity of bamboo with wood, the reviewed articles analyzed the existing models of national standards EC5 [126], Jorissen [137], CSA [127], NDS [87], GB 50005 [128], as well as models developed by Hossain et al. [138], Folz and Filiatrault [125], and Foschi [139], and proposed modified calculation methods suitable for describing the behaviour of the LBL connections. According to the calculated results, there was a trend of conservative predictions based on models of EC5, Jorissen, and SIA 25 [132], while models based on GB 50005 and NDS, Hossain, Folz, and Foschi showed the most accurate results. In many studies of wood connections, the ductile model included in EC5 also proved to be conservative, demonstrating a mode of brittle failure instead of ductile, which could lead to risky situations especially in earthquake-prone regions due to the wrong estimation of the failure mode [68]. Yurrita and Cabrero [68] proposed an optimized method in which the ductile failure mode was based on EC5 without the parameter of the effective number of nails, and brittle failure modes based on the model of Yurrita et al. [142] were considered separately. According to the results, the optimized method reached a total of 90.0% of correct predictions compared to EC5 with 65.0% of positive matches, which in turn calls for the validation of this method for the LBL connections.

4.3 Rods glued-in LBL and wood connections

GIROD-LBL connections have not yet been fully investigated. According to review studies, GIROD-LBL connections have demonstrated 2 failure modes, which were threaded rod fracture and adhesive interface failure. To compare, GIROD-timber connections have the following failure modes: rod tension failure, adhesive failure and cohesive failure of the adhesive, localized timber shear failure, splitting of the timber, and failure of the timber member. Pull-out tests were conducted in the reviewed studies on the behaviour of GIROD-LBL connections, while GIROD-timber connections were experimentally studied through pull-out loading at one or both ends, pull-compression, pull-beam, and pull-pile foundation [143]. The variety of loading configurations calls for further investigation of the capacity of GIROD-LBL connections.

GIROD is a hybrid system that comprises at least three materials such as adhesive, wood or bamboo, and rods, therefore, it is necessary to study the influence of these factors on the mechanical properties of GIROD-LBL connections. For GIROD-LBL connections, two-component epoxy resin was used in the reviewed studies, while commonly used adhesives for GIROD-timber connections were epoxies, polyurethanes, and phenol-resorcinol based adhesives [114]. The impact of glue-line thickness should be studied in terms of GIROD-LBL applications, although, some studies stated that in terms of GIROD-timber applications, it was an important parameter [123], while others reported no significant effect [144,145]. Considering the influence of types of adhesives and species of bamboo on the basic mechanical properties of LBL, it is necessary to conduct further research on their impact in a view of GIROD-LBL applications. Thus, the influence of such factors on the behaviour of GIROD-LBL as different types of rods, adhesives, bamboo species, and environmental conditions remain relevant.

5 Conclusion

Similar to timber connections, it was concluded, that the bearing strength of LBL connections had a strong correlation with material properties, fastener geometries, end and edge distances, spacing and number of fasteners, and loading configuration. However, LBL joints turned out to be stiff and brittle compared to wood connections. Since LBL connections fail in a brittle manner, the ductility of LBL structures should be provided by the proper design of connections.

Considering the sheathing-to-framing connections, LBL panels have similar behaviour to traditional OSB panels and plywood under lateral loads. Due to its density, LBL copes with energy distribution better than conventional materials, which makes it the best for use in seismically hazardous areas. According to the results, the diameter of the screw and the distance between the screws and the nails significantly affected the behaviour of the panels, while the influence of the wall aspect ratio was not observed. In addition to the effect of the thickness, direction, and shape of the lamina, previous studies have noted the influence of the species, glue type, growth portion, and type of processing on the basic physical and mechanical properties of the material. From this, it follows that it is necessary to confirm the influence of these factors on the behaviour of LBL connections.

Similar to wood, bamboo is also an anisotropic material; its connection failure is characterized by splitting caused by the formation of cracks at the location of maximum shear stress. In contrast, failure in timber is generally caused by the formation of a crack at the location of maximum tensile strength perpendicular to grain. According to different failure mechanisms, it is impossible to directly apply timber design rules for splitting prevention in bamboo structures. Therefore, the need for methods predicting the behaviour of bamboo connections is still important. Moreover, the differences in connection performance of caramelized and bleached bamboo call for further investigation of treatment and processing methods' effects on LBL connections.

According to the reviewed studies, LBL has great potential and can serve as a worthy alternative to conventional building materials. Nowadays, the number of tests on LBL connections is far from enough compared with timber structures, so modern practitioners are not fully aware of the structural applications of LBL connections. Some of the studies adopted an insufficient number of samples in order to obtain a preliminary characterization of bamboo-based connections, which led to high COV values, and 95% of reliability could not be achieved. Therefore, it is inevitable to carry out more comprehensive experiments to explore unique bamboo-based factors affecting the behaviour of LBL connections and establish design standards similar to those in use for timber. According to studies, most of the connections failure occurred in LBL itself instead of the connection area, thus, more studies should be held to improve the load-carrying capacity and splitting resistance of LBL.

Funding Statement: The research work presented in this paper is supported by the National Natural Science Foundation of China (Nos. 51878354 & 51308301), the Natural Science Foundation of Jiangsu Province (Nos. BK20181402 & BK20130978), Six talent peak high-level projects of Jiangsu Province (No. JZ029), and Qinglan Project of Jiangsu Higher Education Institutions. Any research results expressed in this paper are those of the writer(s) and do not necessarily reflect the views of the foundations.

Conflicts of Interest: The authors declare that they have no conflicts of interest to report regarding the present study.

References

[1] Arbelaez J, Correal J. Racking performance of traditional and non-traditional engineered bamboo shear walls. Key Eng Mater 2012;517:171–8. https://doi. org/10.4028/www.scientific.net/kem.517.171.
[2] Richard M, Gottron J, Harries K, Ghavami K. Experimental evaluation of longitudinal splitting of bamboo flexural components. Proc Inst Civil Eng - Struct Build 2016;170:1–10. https://doi.org/10.1680/jstbu.16.00072.
[3] Zea Escamilla E, Archila H, Nuramo D, Trujillo D. Bamboo: an engineered alternative for buildings in the Global South. Bioclim Arch Warm Clim 2019: 397–414. https://doi.org/10.1007/978-3-030-12036-8_15.
[4] Harries K, Morrill P, Gauss C, Flower C, Akinbade Y, Trujillo D. Screw withdrawal capacity of full-culm P. edulis bamboo. Constr Build Mater 2019;216:531–41. https://doi.org/10.1016/j.conbuildmat.2019.05.009.

[5] Xiao Y, Li L, Yang RZ. Long-term loading behavior of a full-scale glubam bridge Model. J Bridg Eng 2014;19. https://doi.org/10.1061/(asce)be.1943- 5592.0000600.

[6] Liu KW, Jayaraman D, Shi YJ, Harries K, Yang J, Jin W, et al. Bamboo: a very sustainable construction material" - 2021 International Online Seminar summary report. Sustain Struct 2022;2(1):000015. https://doi.org/10.54113/j. sust.2022.000015.

[7] Lee AWC, Chen G, Tainter FH. Comparative treatability of Moso bamboo and southern pine with CCA preservative using a commercial schedule. Bioresour Technol 2001;77:87–8. https://doi.org/10.1016/s0960-8524(00)00145-0.

[8] Fang CH, Jiang ZH, Sun ZJ, Liu HR, Zhang XB, Zhang R, et al. An overview on bamboo culm flattening. Constr Build Mater 2018;171:65–74. https://doi.org/ 10.1016/j.conbuildmat.2018.03.085.

[9] Mahdavi M, Clouston PL, Arwade SR. Development of laminated bamboo lumber: review of processing, performance, and economical considerations. J Mater Civ Eng 2011;23:1036–42. https://doi.org/10.1061/(Asce)Mt.1943-5533.0000253.

[10] Lei WC, Zhang Y, Yu WJ, et al. The adsorption and desorption characteristics of Moso bamboo induced by heat treatment. J For Eng 2021;6(3):41–6. https://doi. org/10.13360/j.issn.2096-1359.202010008.

[11] Liu HR, Yang XM, Zhang XB, Su Q, Zhang F, Fei B. The tensile shear bonding property of flattened bamboo sheet. Journal of Forestry Engineering 2021;6(1): 68–72. https://doi.org/10.13360/j.issn.2096-1359.202005029.

[12] Escamilla EZ, Habert G, Daza JFC, Archilla HF, Fernandez JSE, Trujillo D. Industrial or Traditional Bamboo Construction? Comparative Life Cycle Assessment (LCA) of Bamboo-Based Buildings. Sustainability 2018;10. https:// doi.org/10.3390/su10093096.

[13] Liu J, Zhou AP, Sheng BL, Liu YY. Sun L.W.Effect of temperature on short-term compression creep property of bamboo scrimber. Journal of Forestry Engineering 2021;6(2):64–9. https://doi.org/10.13360/j.issn.2096-1359.202006003.

[14] Xiao F, Wu YQ, Zuo YF, Peng L, Li WH, Sun XD. Preparation and bonding performance evaluation of bamboo veneer/foam aluminum composites. Journal of Forestry Engineering 2021;6(3):35–40. https://doi.org/10.13360/j.issn.2096- 1359.202009024.

[15] Li Z, Chen C, Mi R, Gan W, Dai J, Jiao M, et al. A strong, tough, and scalable structural material from fast-growing bamboo. Adv Mater 2020;32:1906308. https://doi.org/10.1002/adma.201906308.

[16] Huang ZR, Chen ZF, Huang DS, Zhou AP. The ultimate load-carrying capacity and deformation of laminated bamboo hollow decks: experimental investigation and inelastic analysis. Constr Build Mater 2016;117:190–7. https://doi.org/10.1016/ j.conbuildmat.2016.04.115.

[17] Jin XB, Jiang ZH, Wen XW, Zhang R, Qin DC. Flame retardant properties of laminated bamboo lumber treated with monoammonium phosphate (MAP) and boric acid/borax (SBX) compounds. BioResources 2017;12:5071–85. https://doi. org/10.15376/biores.12.3.5071-5085.

[18] Yang G, Kun W. Evaluation on the application of GLB structures. J Mater Sci Chem 2020;8(5):21–37. https://doi.org/10.4236/msce.2020.85003.

[19] Li H, Xuan Y, Xu B, Li S. Bamboo application in civil engineering field. J For Eng 2020;5:1–10. https://doi.org/10.13360/j.issn.2096-1359.202003001.

[20] Su J, Li H, Xiong Z, Lorenzo R. Structural design and construction of an office building with laminated bamboo lumber. Sustainable Structures 2021;1(2): 000010. https://doi.org/10.54113/j.sust.2021.000010.

[21] Yu HQ, Jiang ZH, Hse CY, Shupe TF. Selected physical and mechanical properties of Moso bamboo (Phyllostachys Pubescens). J Trop For Sci 2008;20:258–63. https://www.jstor.org/stable/23616702.

[22] Chung KF, Yu WK. Mechanical properties of structural bamboo for bamboo scaffoldings. Eng Struct 2002;24:429–42. https://doi.org/10.1016/S0141-0296 (01)00110-9.

[23] Lorenzo R, Godina M, Mimendi L. Determination of the physical and mechanical properties of moso, guadua and oldhamii bamboo assisted by robotic fabrication. J Wood Sci 2020;66(20). https://doi.org/10.1186/s10086-020-01869-0.

[24] Lo TY, Cui HZ, Tang PWC, Leung HC. Strength analysis of bamboo by microscopic investigation of bamboo fibre. Constr Build Mater 2008;22:1532–5. https://doi. org/10.1016/j.conbuildmat.2007.03.031.

[25] Lou Z, Yuan C, Li Y, Shen D, Yang L, Liu J, et al. Effect of saturated steam treatment on the chemical composition and crystallinity properties of bamboo bundles. J For Eng 2020;5:29–35. https://doi.org/10.13360/j.issn.2096- 1359.201905014.
[26] Lou Z, Yang L, Zhang A, Shen D, Liu J, Yuan C, et al. Influence of saturated steam heat treatment on the bamboo color. J For Eng 2020;5:38–44. https://doi.org/ 10.13360/j.issn.2096-1359.201906044.
[27] Dixon PG, Gibson LJ. The structure and mechanics of Moso bamboo material. J R Soc Interface 2014;11:20140321. https://doi.org/10.1098/rsif.2014.0321.
[28] Vilanova A, Fernandez-G ´ omez ´ J, Landsberger GA. Evaluation of the mechanical properties of self compacting concrete using current estimating models Estimating the modulus of elasticity, tensile strength, and modulus of rupture of self compacting concrete. Constr Build Mater 2011;25:3417–26. https://doi.org/ 10.1016/j.conbuildmat.2011.03.033.
[29] Chow A, Ramage MH, Shah DU. Optimising ply orientation in structural laminated bamboo. Constr Build Mater 2019;212:541–8. https://doi.org/ 10.1016/j.conbuildmat.2019.04.025.
[30] Deng JC, Chen FM, Li HD, Wang G, Shi SQ. The effect of PF/PVAC weight ratio and ambient temperature on moisture absorption performance of bamboo-bundle laminated veneer lumber. Polym Compos 2016;37:955–62. https://doi.org/ 10.1002/pc.23255.
[31] Deng J, Wei X, Zhou H, Wang G, Zhang S. Inspiration from table tennis racket: preparation of rubber-wood-bamboo laminated composite (RWBLC) and its response characteristics to cyclic perpendicular compressive load. Compos Struct 2020;241:112135. https://doi.org/10.1016/j.compstruct.2020.112135.
[32] Chen G, Yu YF, Li X, He B. Mechanical behavior of laminated bamboo lumber for structural application: an experimental investigation. Eur J Wood Wood Prod 2020;78:53–63. https://doi.org/10.1007/s00107-019-01486-9.
[33] Sharma B, Bauer H, Schickhofer G, Ramage MH. Mechanical characterisation of structural laminated bamboo. Proc Inst Civ Eng: Struct 2017;170:250–64. https://doi.org/10.1680/jstbu.16.00061.
[34] Yu Y, Huang X, Yu W. A novel process to improve yield and mechanical performance of bamboo fiber reinforced composite via mechanical treatments. Compos B Eng 2014;56:48–53. https://doi.org/10.1016/j. compositesb.2013.08.007.
[35] Park SH, Jang JH, Wistara Nyoman J, Hidayat W, Lee M, Febrianto F. Anatomical and physical properties of indonesian bamboos carbonized at different temperatures. J Korean Wood Sci Technol 2018;46:656–69. https://doi.org/ 10.5658/wood.2018.46.6.656.
[36] Li Y, Lou Z. Progress of bamboo flatten technology research. J For Eng 2021;6: 14–23. https://doi.org/10.13360/j.issn.2096-1359.202012021.
[37] Li HT, Wu G, Xiong ZH, Corbi I, Corbi O, Xiong XH, et al. Length and orientation direction effect on static bending properties of laminated Moso bamboo. Eur J Wood Wood Prod 2019;77:547–57. https://doi.org/10.1007/s00107-019-01419- 6.
[38] Li HT, Deeks AJ, Zhang QS, Wu G. Flexural Performance of Laminated Bamboo Lumber Beams. BioResources 2016;11:929–43. https://doi.org/10.15376/ biores.11.1.929-943.
[39] Jorissen AJM, Voermans J, Jansen MH. Glued-laminated bamboo: Node and joint failure in bamboo laminations in tension. J Bamboo Ratt 2007;6(3–4):137–44.
[40] Ni L, Zhang XB, Liu HR, Sun ZJ, Song GN, Yang LM, et al. Manufacture and mechanical properties of glued bamboo laminates. BioResources 2016;11: 4459–71. https://doi.org/10.15376/biores.11.2.4459-4471.
[41] Sharma B, Gatoo A, Ramage MH. Effect of processing methods on the mechanical properties of engineered bamboo. Constr Build Mater 2015;83:95–101. https:// doi.org/10.1016/j.conbuildmat.2015.02.048.
[42] Forest Products Laboratory. Wood handbook wood as an engineering material. General Technical Report FPL-GTR-282. Madison, WI: U.S. Department of Agriculture, Forest Service, Forest Products Laboratory, 2021. 543 p.
[43] Zhang XL, Que YL, Wang XM, Li ZR, Zhang LL, Que ZL, et al. Experimental behavior of laminated veneer lumber with round holes, with and without reinforcement. BioResources 2018;13:8899–910. https://doi.org/10.15376/ biores.13.4.8899-8910.

[44] Huang YX, Ji YH, Yu WJ. Development of bamboo scrimber: a literature review. J Wood Sci 2019;65:25. https://doi.org/10.1186/s10086-019-1806-4.
[45] Marx CM, Moody RC. Bending strength of shallow glued-laminated beams of a uniform grade. Res. Pap. FPL-380. Madison, WI: U.S. Department of Agriculture, Forest Service, Forest Products Laboratory, 1981. 19 p. https://doi.org /10.2737/FPL-RP-380.
[46] Sousa HS, Branco JM, Lourenco PB. Glulam mechanical characterization. Adv Mater Forum Vi, Pts 1 and 2 2013;2(730–732):994–9. https://doi.org/10.4028/ www.scientific.net/MSF.730-732.994.
[47] Hugot F, Cazaurang G. Mechanical properties of an extruded wood plastic composite. Mec Ind 2009;10:519–24. https://doi.org/10.1051/meca/2010010.
[48] Verma CS, Chariar VM. Development of layered laminate bamboo composite and their mechanical properties. Compos B Eng 2012;43:1063–9. https://doi.org/ 10.1016/j.compositesb.2011.11.065.
[49] Dauletbek A, Li H, Lorenzo R, Corbi I, Corbi O, Ashraf M. A review of basic mechanical behavior of laminated bamboo lumber. J Renewable Mater 2022;10: 273–300. https://doi.org/10.32604/jrm.2022.017805.
[50] Wei X, Chen F, Wang G. Flexibility characterization of bamboo slivers through winding-based bending stiffenss method. J For Eng 2020;5:48–53. https://doi. org/10.13360/j.issn.2096-1359.201905046.
[51] Wang R, Xiao Y, Li Z. Lateral loading performance of lightweight glubam shear walls. J Struct Eng 2017;143. https://doi.org/10.1061/(asce)st.1943- 541X.0001751.
[52] Wang R, Wei SQ, Li Z, Xiao Y. Performance of connection system used in lightweight glubam shear wall. Constr Build Mater 2019;206:419–31. https://doi. org/10.1016/j.conbuildmat.2019.02.081.
[53] Yang RZ, Xiao Y. Experimental study of glubam single-bolted joint loaded by tension. Key Eng Mater 2012;517:34–42. https://doi.org/10.4028/www. scientific.net/kem.517.34.
[54] Li TY, Shan B, Xiao Y, Guo YR, Zhang MP. Axially loaded single threaded rod glued in glubam joint. Constr Build Mater 2020;244. https://doi.org/10.1016/j. conbuildmat.2020.118302.
[55] Xiao Y, Shan B, Yang RZ, Li Z, Chen J. In: Aicher S, Reinhardt HW, Garrecht H, editors. Materials and Joints in Timber Structures. RILEM Bookseries, Vol. 9. Dordrecht: Springer; 2014. https://doi.org/10.1007/978-94-007-7811-5_54.
[56] Li Z, Zhang J, Wang R, Monti G, Xiao Y. Design embedment strength of plybamboo panels used for glubam. J Mater Civ Eng 2020;32. https://doi.org/ 10.1061/(asce)mt.1943-5533.0003128.
[57] Cui ZY, Xu M, Chen ZF, Wang F. Experimental study on bearing capacity of bolted steel-PSB-steel connections. Eng Mech 2019;36(1):96–103,118. https://doi.org/ 10.6052/j.issn.1000-4750.2017.11.0792.
[58] Cui Z, Wang F, Xu M, Chen Z. Experimental study on embedding strength of bamboo scrimber parallel to grain at high temperatures. J Southeast Univ 2017; 47:1174–9. https://doi.org/10.3969/j.issn.1001-0505.2017.06.015.
[59] Chen Y, Li H, Yang D, Lorenzo R, Yuan C. Experimental evaluation of the dowelbearing strength of laminated flattened-bamboo lumber perpendicular to grain. Constr Build Mater 2022;350:128791. https://doi.org/10.1016/j. conbuildmat.2022.128791.
[60] Wang S, Li H, Cheng G, Xiong Z, Ashraf M. Mechanical behavior of bolted steel laminated bamboo lumber connections loaded perpendicular to grain. Constr Build Mater 2022;345:128302. https://doi.org/10.1016/j. conbuildmat.2022.128302.
[61] Xiao Y, Chen G, Feng L. Experimental studies on roof trusses made of glubam. Mater Struct 2014;47:1879–90. https://doi.org/10.1617/s11527-013-0157-7.
[62] Chen C, Ye ZN, Yu XH, Tor O, Zhang JL. Cyclic behavior of self-tapping screwed laminated bamboo lumber connections subjected to cycle loadings. BioResources 2019;14:7958–76. https://doi.org/10.15376/biores.14.4.7958-7976.
[63] Dauletbek A, Li H, Xiong Z, Lorenzo R. A review of mechanical behavior of structural laminated bamboo lumber. Sustain Struct 2021;1(1):000004. https:// doi.org/10.54113/j.sust.2021.000004.
[64] Ramage M, Sharma B, Bock M, Gatoo ´ A, Mulligan H. Engineered bamboo: state of the art. Proc Inst Civ Eng: Constr Mater 2015;168:57–67. https://doi.org/ 10.1680/coma.14.00020.
[65] Gatoo ´ A, Sharma B, Bock M, Mulligan H, Ramage M. Sustainable structures: bamboo standards and building codes. Proc Inst Civ Eng: Eng Sustain 2014;167: 189–96. https://doi.org/10.1680/ensu.14.00009.

[66] Dis´en K, Clouston P. Building with bamboo: a review of culm connection technology. J Green Build 2013;8:83–93. https://doi.org/10.3992/jgb.8.4.83.
[67] Hong C, Lorenzo R, Wu G, Corbi I, Corbi O, Xiong Z, et al. Review on connections for original bamboo structures. J Renew Mater 2019;7:713–30. https://doi.org/ 10.32604/jrm.2019.07647.
[68] Yurrita M, Cabrero JM. On the need of distinguishing ductile and brittle failure modes in timber connections with dowel-type fasteners. Eng Struct 2021;242. https://doi.org/10.1016/j.engstruct.2021.112496.
[69] Ashraf M, Hasan MJ, Al-Deen S. Semi-rigid behaviour of stainless steel beam-tocolumn bolted connections. Sustain Struct 2021;1(1):000002. https://doi.org/ 10.54113/j.sust.2021.000002.
[70] M´endez Quintero MA, Takeuchi Tam CP, Li H. Structural analysis of a Guadua bamboo bridge in Colombia. Sustain Struct 2022;2(2):000020. https://doi.org/ 10.54113/j.sust.2022.000020.
[71] Mimendi L, Lorenzo R, Li H. An innovative digital workflow to design, build and manage bamboo structures. Sustain Struct 2022;2(1):000011. https://doi.org/ 10.54113/j.sust.2022.000011.
[72] Dolan JD, Madsen B. Monotonie and cyclic tests of timber shear walls. Can J Civ Eng 1992;19:415–22. https://doi.org/10.1139/l92-050.
[73] Lebeda D. The effect of hold-down misplacement on the strength and stiffness of wood shear walls. Pract Period Struct Des Constr 2005;10(2):79–87. https://doi. org/10.1061/(asce)1084-0680(2005)10:2(79).
[74] Heine CP, Dolan J. Dynamic performance of perforated light-frame shear walls with various end restraints. For Prod J 2001;51:65–72.
[75] Salenikovich A, Dolan J. The racking performance of shear walls with various aspect ratios. Part 2. Cyclic tests of fully anchored walls. For Prod J 2003;53: 37–45.
[76] Jones SN, Fonseca FS. Capacity of oriented strand board shear walls with overdriven sheathing nails. J Struct Eng 2002;128:898–907. https://doi.org/ 10.1061/(asce)0733-9445(2002)128:7(898).
[77] Gatto K, Uang CM. Effects of loading protocol on the cyclic response of woodframe shearwalls. J Struct Eng 2003;129:1384–93. https://doi.org/ 10.1061/(asce)0733-9445(2003)129:10(1384).
[78] Cassidy ED, Davids WG, Dagher HJ, Gardner DJ. Performance of wood shear walls sheathed with FRP-reinforced OSB panels. J Struct Eng 2006;132:153–63. https://doi.org/10.1061/(asce)0733-9445(2006)132:1(153).
[79] Lindt JW, Potts A. Shake table testing of a superelastic shape memory alloy response modification device in a wood shearwall. J Struct Eng 2008;134: 1343–52. https://doi.org/10.1061/(asce)0733-9445(2008)134:8(1343).
[80] Sun YH, Jiang ZH, Zhang XB, Sun ZJ, Liu HR. Behavior of glued laminated bamboo and bamboo-oriented strand board sheathing-to-framing connections. Eur J Wood Wood Prod 2019;77:1189–99. https://doi.org/10.1007/s00107-019- 01454-3.
[81] Sinha A, Miyamoto BT. Lateral load carrying capacity of laminated bamboo lumber and oriented strand board connections. J Mater Civ Eng 2014;26:741–7. https://doi.org/10.1061/(asce)mt.1943-5533.0000848.
[82] Li Z, Xiao Y, Wang R, Monti G. Studies of nail connectors used in wood frame shear walls with ply-bamboo sheathing panels. J Mater Civ Eng 2014;27: 04014216. https://doi.org/10.1061/(asce)mt.1943-5533.0001167.
[83] Echeverry JS, Correal JF. Cyclic behavior of laminated Guadua mat sheathing-toframing connections. Constr Build Mater 2015;98:69–79. https://doi.org/ 10.1016/j.conbuildmat.2015.08.109.
[84] ASTM D1761 (2012) Standard test methods for mechanical fasteners in wood. West Conshohocken, PA, USA: ASTM International; 2012.
[85] ISO 16670 (2003) Timber structures – joints made with mechanical fasteners – Quasi-static reversed cyclic test method. Geneva: International Organization for Standardization.
[86] Dolan J. Proposed test method for dynamic, properties of connections assembled with mechanical fasteners. J Test Eval 1994;22(6). https://doi.org/10.1520/ jte11859J.
[87] American Forest, Paper Association. ANSI/AF&PA NDS-2012 National Design Specification for Wood Construction. Washington, D.C: AF&PA; 2012.

[88] Varela S, Correal J, Yamin L, Ramirez F. Cyclic performance of glued laminated Guadua bamboo-sheathed shear walls. J Struct Eng 2013;139:2028–37. https:// doi.org/10.1061/(asce)st.1943-541X.0000758.
[89] Correal J, Varela S. Experimental study of glued laminated Guadua bamboo panel as an alternative shear wall sheathing material. Key Eng Mater 2012;517:164–70. https://doi.org/10.4028/www.scientific.net/kem.517.164.
[90] Luna P, Takeuchi C. Experimental analysis of frames made with glued laminated pressed bamboo Guadua. Key Eng Mater 2012;517:184–8. https://doi.org/ 10.4028/www.scientific.net/kem.517.184.
[91] Xiao Y, Li Z, Wang R. Lateral loading behaviors of lightweight wood-frame shear walls with ply-bamboo sheathing panels. J Struct Eng 2015;141(3):B4014004. https://doi.org/10.1061/(asce)st.1943-541X.0001033.
[92] Cui ZY, Tu LH, Xu M, Chen ZF, Wang CX. The evaluation of dowel-bearing properties of laminated bamboo parallel to grain. Structures 2020;25:956–64. https://doi.org/10.1016/j.istruc.2020.04.004.
[93] Cui Z, Xu M, Tu L, Chen Z, Hui B. Determination of dowel-bearing strength of laminated bamboo at elevated temperatures. J Build Eng 2020;30. https://doi. org/10.1016/j.jobe.2020.101258.
[94] Li J, Zhou A. Mechanical behavior of laminated bamboo lumber dowel-type connection. Adv Struct Eng 2019;23:65–73. https://doi.org/10.1177/ 136943321986609.
[95] Ramirez F, Correal JF, Yamin LE, Atoche JC, Piscal CM. Dowel-bearing strength behavior of glued laminated Guadua bamboo. J Mater Civ Eng 2012;24:1378–87. https://doi.org/10.1061/(asce)mt.1943-5533.0000515.
[96] Khoshbakht N, Clouston PL, Arwade SR, Schreyer AC. Computational modeling of laminated veneer bamboo dowel connections. J Mater Civ Eng 2018;30. https:// doi.org/10.1061/(asce)mt.1943-5533.0002135.
[97] Reynolds T, Sharma B, Harries K, Ramage M. Dowelled structural connections in laminated bamboo and timber. Compos B Eng 2016;90:232–40. https://doi.org/ 10.1016/j.compositesb.2015.11.045.
[98] Chen G, Jiang H, Yu YF, Zhou T, Wu J, Li X. Experimental analysis of nailed LBLto-LBL connections loaded parallel to grain. Mater Struct 2020;53. https://doi. org/10.1617/s11527-020-01517-5.
[99] Chen G, Yang WQ, Zhou T, Yu YF, Wu J, Jiang H, et al. Experiments on laminated bamboo lumber nailed connections. Constr Build Mater 2021;269. https://doi. org/10.1016/j.conbuildmat.2020.121321.
[100] Cui ZY, Tu LH, Xu M, Chen ZF, Xu QF. Experimental investigation on the loadcarrying capacity of steel-to-laminated bamboo dowel connection I: single fastener with slotted-in steel plate under tension. Adv Civ Eng 2021. https://doi. org/10.1155/2021/6683589.
[101] Tang G, Yin LF, Li ZJ, Li Y, You LG. Structural behaviors of bolted connections using laminated bamboo and steel plates. Structures 2019;20:324–39. https:// doi.org/10.1016/j.istruc.2019.04.001.
[102] Leng Y, Xu Q, Harries KA, Chen L, Liu K, Chen X. Experimental study on mechanical properties of laminated bamboo beam-to-column connections. Eng Struct 2020;210. https://doi.org/10.1016/j.engstruct.2020.110305.
[103] Castaneda H, Bjarnadottir S. Analysis of the bolted connection of a bamboo composite I-shaped beam subjected to bending. Procedia Eng 2016;145:796–803. https://doi.org/10.1016/j.proeng.2016.04.104.
[104] ASTM D5764 (2013). Standard test method for evaluating dowel-bearing strength of wood and wood-based products. West Conshohocken, PA, USA: ASTM International; 2013.
[105] BSI (2007) Timber structures. Test methods. Determination of embedment strength and foundation values for dowel type fasteners. ASTM International, West Conshohocken, PA, USA, 2007. A. Dauletbek et al. Composite Structures 313 (2023) 116898 20
[106] ASTM D2915 (1999) Standard practice for evaluating allowable properties for grades of structural lumber. ASTM International, West Conshohocken, PA, USA, 1999.
[107] ASTM D5652 (2015) Standard test methods for single-bolt connections in wood and wood-based products, ASTM International, West Conshohocken, PA, USA, 2015.
[108] ASTM E2126-09 (2015) Standard test methods for cyclic (reversed) load test for shear resistance of vertical elements of the lateral force resisting systems for buildings. ASTM International, West Conshohocken, PA, USA, 2015.

[109] Saliklis E, Falk R. Correlating off-axis tension tests to shear modulus of woodbased panels. J Struct Eng 2000;126(5). https://doi.org/10.1061/(asce)0733- 9445(2000)126:5(621).
[110] DIN EN 302-2:1992-08 (1979) Adhesives for load-bearing timber structures; test methods; part 2: determination of resistance to delamination (laboratory method). Deutsches Institut für Normung e.V., Berlin, Germany, 1979.
[111] Aicher S, Gustafsson P, Wolf M. Load displacement and bond strength of glued-in rods in timber influenced by adhesive, wood density, rod slenderness and diameter. In: Proceedings of the 1st RILEM Symposium on timber engineering, Stockholm, 1999, pp. 369–78.
[112] Bengtsson C, Johansson CJ. GIROD: Glued in rods for timber structures. SP report, Sveriges provnings-och Forskningsinstitut (SP), Borås, 2002; 2002:26.
[113] Kemmsies M. Comparison of bond lines in glulam beams adhered with a phenolresorcinol-formaldehyde (PRF) and one-component polyurethane (PUR) after fire exposure. In: Proceedings of the First RILEM Symposium on Timber Engineering. RILEM Publications SARL; 1999. p. 399–408.
[114] Davis G. The performance of adhesive systems for structural timbers. Int J Adhes Adhes 1997;17:247–55. https://doi.org/10.1016/S0143-7496(97)00010-9.
[115] Kamke FA, Lee JN. Adhesive penetration in wood-a review. Wood Fiber Sci 2007; 39(2):205–20.
[116] Gonzales E, Tannert T, Vallee T. The impact of defects on the capacity of timber joints with glued-in rods. Int J Adhes Adhes 2016;65:33–40. https://doi.org/ 10.1016/j.ijadhadh.2015.11.002.
[117] McBain JW, Hopkins DG. On Adhesives and Adhesive Action. J Phys Chem 1925; 29:188–204. https://doi.org/10.1021/j150248a008.
[118] Yan Y, Liu HR, Zhang XB, Wu H, Huang Y. The effect of depth and diameter of glued-in rods on pull-out connection strength of bamboo glulam. J Wood Sci 2016;62:109–15. https://doi.org/10.1007/s10086-015-1516-5.
[119] ASTM D1761-88 (1998) Standard test methods for mechanical fasteners in wood. ASTM International, West Conshohocken, PA, USA, 1998.
[120] Zhang XB, Jiang ZH, Fei BH, Fang CH, Liu HR. Experimental performance of threaded steel glued into laminated bamboo. Constr Build Mater 2020;249. https://doi.org/10.1016/j.conbuildmat.2020.118780.
[121] Riberholt H. Glued bolts in glulam-proposals for CIB code. Proposal for CIB Code. In: Proc. of the CIB-W18. Meeting, 1988.
[122] The European Standard EN 1995-2:1997, Eurocode 5: Design of Timber Structures-Part 2: Bridges, 1997.
[123] Feligioni L, Lavisci P, Duchanois G, De Ciechi M, Spinelli P. Influence of glue rheology and joint thickness on the strength of bonded-in rods. Holz Roh Werkst 2003;61:281–7. https://doi.org/10.1007/s00107-003-0387-4.
[124] Deutsches Institut für Normung e.V. DIN, Norm 1052:2008-12 Entwurf, Berechnung and Bemessung von Holzbauwerken, DIN, Berlin, 2008.
[125] Folz B, Filiatrault A. Cyclic analysis of wood shear walls. J Struct Eng 2001;127: 433–41. https://doi.org/10.1061/(asce)0733-9445(2001)127:4(433).
[126] The European Standard EN 1995-1-1:2004(E), Eurocode 5: Design of Timber Structures-Part 1-1: General-Common Rules and Rules for Buildings, 2004.
[127] CSA O86 (2009) Engineering design in wood. [128] GB 50005 (2017) Standard for design of timber structures.
[129] Architectural Institute of Japan, Design Guidelines for Limit State of Wood Structure, 2002.
[130] Karacabeyli E, Lau P, Deacon W, Henderson CR, Meakes FV. Design rated oriented strandboard in CSA standards. Can J Civ Eng 1996;23:431–43. https://doi.org/ 10.1139/l96-047.
[131] Ministry of Housing and Urban-Rural Construction of the People's Republic of China, GB/T 50708-2012, Technical Code of Glued Laminated Timber Structures, China Architecture Industry Press, Beijing, 2012.
[132] SIA 265:2012 Timber Structures. Swiss Society of Engineers and Architects (SIA), Zurich, Switzerland, 2012.
[133] Cramer C. Load Distribution in Multiple-Bolt Tension Joints. J Struct Div ASCE 1968;94:1101–17.

[134] Lantos G. Load distribution in a row of fasteners subjected to lateral load. Wood Sci 1969;1:129–36.
[135] Wilkinson TL. Load Distribution among Bolts Parallel to Load. J Struct Eng 1986; 112:835–52. https://doi.org/10.1061/(asce)0733-9445(1986)112:4(835).
[136] Xu BH, Taazount M, Bouchaïr A, Racher P. Numerical 3D finite element modelling and experimental tests for dowel-type timber joints. Constr Build Mater 2009;23: 3043–52. https://doi.org/10.1016/j.conbuildmat.2009.04.006.
[137] Jorissen A. Double shear timber connections with dowel type fasteners. Heron 1999;44(3).
[138] Hossain A, Popovski M, Tannert T. Group effects for shear connections with selftapping screws in CLT. J Struct Eng 2019;145(8):04019068. https://doi.org/ 10.1061/(asce)st.1943-541X.0002357.
[139] Foschi RO. Load-slip characteristics of nails. Wood Science 1974;7:69–76.
[140] Lau PWC. Rationalizing spacing requirements for nailed wood connections by induced wood splitting. Can J Civ Eng 1992;19:42–846. https://doi.org/10.1139/ l92-095.
[141] Porteous A, Kermani A. Fully overlapping nailed joints with steel gussets in timber structures. J Struct Eng 2005;131(5):806. https://doi.org/10.1061/(asce) 0733-9445(2005)131:5(806).
[142] Yurrita M, Cabrero JM, Quenneville P. Brittle failure in the parallel-to-grain direction of multiple shear softwood timber connections with slotted-in steel plates and dowel-type fasteners. Constr Build Mater 2019;216:296–313. https:// doi.org/10.1016/j.conbuildmat.2019.04.100.
[143] Tlustochowicz G, Serrano E, Steiger R. State-of-the-art review on timber connections with glued-in steel rods. Mater Struct 2011;44(5):997–1020. https:// doi.org/10.1617/s11527-010-9682-9.
[144] Bainbridge R, Mettem C, Harvey K, Ansell M. Bonded-in rod connections for timber structures - development of design methods and test observations. Int J Adhes 2002;22(1):47–59. https://doi.org/10.1016/S0143-7496(01)00036-7.
[145] Broughton JG, Hutchinson AR. Adhesive systems for structural connections in timber. Int J Adhes 2001;21(3):177–86. https://doi.org/10.1016/S0143-7496 (00)00049-X.